LBL-18082

Lawrence Berkeley Laboratory

UNIVERSITY OF CALIFORNIA

RECEIVED
LAWRENCE
BERKELEY LABORATORY

SEP 10 1984

LIBRARY AND
DOCUMENTS SECTION

Materials & Molecular Research Division

THE EFFECT OF COLLISION ENERGY AND VIBRATIONAL EXCITATION ON ENDOTHERMIC ION-MOLECULE REACTIONS

T.P. Turner
(Ph.D. Thesis)

July 1984

TWO-WEEK LOAN COPY

This is a Library Circulating Copy
which may be borrowed for two weeks.

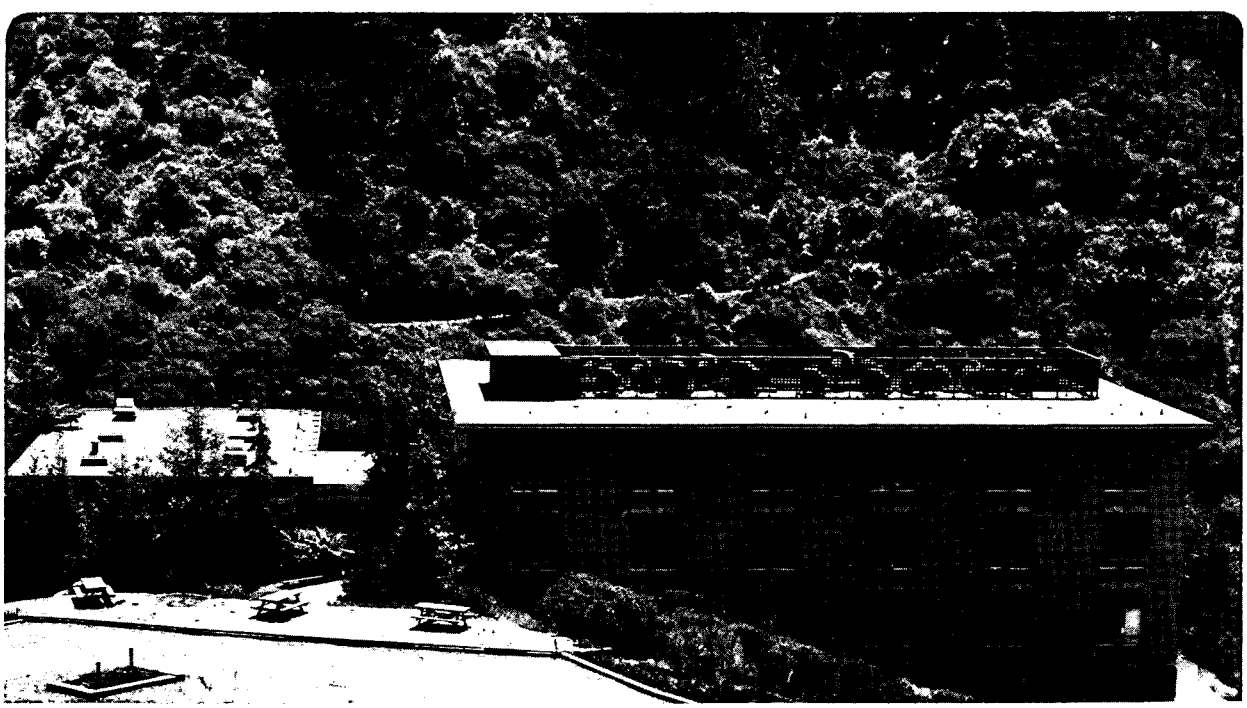

Prepared for the U.S. Department of Energy under Contract DE-AC03-76SF00098

LBL-18082

DISCLAIMER

This document was prepared as an account of work sponsored by the United States Government. While this document is believed to contain correct information, neither the United States Government nor any agency thereof, nor the Regents of the University of California, nor any of their employees, makes any warranty, express or implied, or assumes any legal responsibility for the accuracy, completeness, or usefulness of any information, apparatus, product, or process disclosed, or represents that its use would not infringe privately owned rights. Reference herein to any specific commercial product, process, or service by its trade name, trademark, manufacturer, or otherwise, does not necessarily constitute or imply its endorsement, recommendation, or favoring by the United States Government or any agency thereof, or the Regents of the University of California. The views and opinions of authors expressed herein do not necessarily state or reflect those of the United States Government or any agency thereof or the Regents of the University of California.

LBL-18082

THE EFFECT OF COLLISION ENERGY AND VIBRATIONAL EXCITATION ON ENDOTHERMIC ION-MOLECULE REACTIONS

Thomas P. Turner
(Ph. D. Thesis)

Materials and Molecular Research Division,
Lawrence Berkeley Laboratory and
Department of Chemistry,
University of California,
Berkeley, California 94720 USA

This work was supported by the Director, Office of Energy Research, Office of Basic Energy Sciences, Chemical Sciences Division of the U.S. Department of Energy under Contract No. DE-AC03-76SF00098.

To Mutti and Lati

Table of Contents

ABSTRACT. v

ACKNOWLEDGEMENTS. vii

CHAPTER 1 GENERAL INTRODUCTION

Ion-molecule reaction dynamics. 1

References. 10

CHAPTER 2 EXPERIMENT

Total cross section measurements. 12

References. 21

Figures 22

Tables. 26

CHAPTER 3 H_2^+, HD^+ + He

Introduction. 27

Results and analysis. 31

Discussion. 34

Conclusion. 44

References. 45

Figures 47

Tables. 54

CHAPTER 4 $C_2H_2^+ + H_2$

Introduction. 57

Results and analysis. 61

Discussion. 63

References. 70

Figures 72

Tables. 77

THE EFFECT OF COLLISION ENERGY AND VIBRATIONAL EXCITATION ON ENDOTHERMIC ION-MOLECULE REACTIONS

Thomas P. Turner
(Ph. D. Thesis)

Materials and Molecular Research Division,
Lawrence Berkeley Laboratory and
Department of Chemistry,
University of California,
Berkeley, California 94720 USA

Abstract

This thesis is divided into two major parts. In the first part an experimental study of proton and deuteron transfer in H_2^+ + He and HD^+ + He has been carried out as a function of kinetic and vibrational energy. The data gives evidence that at lower kinetic energies, the spectator stripping mechanism indeed plays an important role when H_2^+ or HD^+ is vibrationally excited. The $H_2^+(v=0)$ reaction has a much smaller cross section than the v=1-4 reactions and seems to go through intimate, small impact parameter collisions involving all the atoms. Investigation of the competition between both the proton and deuteron transfer channels for the HD^+ case, shows that vibrational enhancement towards forming the HeD^+ product falls off sooner with increasing kinetic energy than does the HeH^+ product again in accordance with the spectator stripping model. The higher yield for HeH^+ production at both higher vibrational levels of HD^+ and at lower kinetic energy and the behavior of translational energy dependence of HeH^+ seems to indicate the importance of the induced orientation of HD^+ during the collision with He. Because of the displacement of the center of mass

from the center of charge in HD^+, the charge induced dipole interaction between He and HD^+ tends to swing the H atom more towards He during the approach of He and HD^+.

The second half of this thesis examines the relative efficiencies between the excitation of C-C stretching vibration and collision energy on the promotion of the H atom transfer reaction of $C_2H_2^+ + H_2 \rightarrow C_2H_3^+ + H$. At low collision energies the reaction is strongly vibrationally enhanced in agreement with previous thermal energy studies. Translational energy was found to be not as effective as exciting the C-C stretching vibration in promoting the reaction. The results indicate that the H atom transfer from H_2 to the C atom should have a late barrier, but the C-C stretching vibration of $C_2H_2^+$ is apparently coupled to the reaction coordinate. Because the C-C bond in $C_2H_3^+$ is expected to be longer than that of $C_2H_2^+$, vibrational energy added to the C-C bond might reduce the barrier for H atom transfer from H_2 to a C atom in $C_2H_2^+$.

Acknowledgements

My deepest thanks certainly go to my scientific father Yuan Lee. I would also like to thank Bruce Mahan for letting me start my graduate career in his group. I have had the pleasure of working with many fine people; in particular I wish to acknowledge my coworkers Steve Hansen, Scott Anderson, and Odile Dutuit. Finally I would like to thank the Fannie and John Hertz Foundation for their most generous support for my entire schooling in Berkeley. This work was supported by the Director, Office of Energy Research, Office of Basic Energy Sciences, Chemical Sciences Division of the U.S. Department of Energy under Contract No. DE-AC03-76SF00098.

CHAPTER 1 GENERAL INTRODUCTION

Ion-molecule reaction dynamics

It is the intent of our research group to study the details of chemical reaction dynamics. Ion-molecule reactions have been studied by a variety of methods including mass spectrometry, flowing afterglow, ion cyclotron resonance, and crossed beams.[1,2] Most of these studies have used electron impact ionization for the production of reactant ions. The disadvantage with electron impact ionization is that the ions are produced with a broad range of vibrational energies which may drastically influence the reaction. Using photoionization ions can be produced with some degree of state selection. Chupka, et. al. had pioneered the use of photoionization in ion-molecule reactions;[3] he prepared vibrationally pure H_2^+ ions for use in the reaction $H_2^+ + H_2 \rightarrow H_3^+ + H$. The reaction was found to be slightly less probable with increasing vibrational energy at thermal collision energy. The trend reverses itself as the collision energy is raised past 1 eV. Because photon fluxes are usually smaller than electron emission currents (10^{10} photons/sec for this experiment versus 10^{15} - 10^{16} electrons/sec for emission currents up to 1 mA) and photoionization cross sections are generally lower than electron impact ionization cross sections, photoion intensities can be somewhat limited. See references 4 and 5 for ionization cross sections of H_2 and N_2 as examples.

The best possible reaction to study would be if one were to specify all the reactants' quantum states, pre- and post-collisional

angular momenta and kinetic energies, and products' quantum states. The cross section for such a detailed reaction would then be measured. Obviously such detail is quite impractical, but one can attempt to study a reaction with as much control (state selection) as possible, for instance using photoionization over electron impact ionization as stated above. The degree of state selection is always at the cost of some reactant or product intensity. Besides knowledge of the molecular system's quantum internal states, one needs to have some information about the collisional angular momentum and kinetic energy states. A crossed beams experiment gives one dynamical knowledge of the reaction, that is, angular and energy resolved differential cross sections. However, because the products are spread throughout velocity space, intense beams must be used or the reaction must be confined to some kinematically acceptable portion of velocity space. Integrating differential cross sections or collecting all scattered products gives one the integral or total cross section as described in this thesis. Here a smaller cross section reaction or a reaction using less intense reactants may be studied at the cost of some dynamical information.

Ultimately, with experimental data in hand, the experimental observations might be understood from the nature of the potential energy surface (PES) comparing the data against theoretical scattering calculations. These calculations can be carried out with various levels of sophistication from classical and semi-classical to quantum treatments. In order to calculate trajectories, a PES is required. How well theoretical predictions match experimental results depends on the accuracy of the PES as well as the method by which the scattering

calculations are performed. A surface can be generated by ab initio, diatomic-in-molecules (DIM), etc. methods.[6] To compute ab initio surfaces, a variety of methods may be used to solve or approximate the Hartree-Fock equations. For polyatomic systems where exact solution of the Hartree-Fock equations is too difficult (in terms of complexity, computational time requirements, etc.), one may use the self consistent field (SCF) method where one uses an incomplete, but useful set of basis functions with which to calculate the energy eigenstates. The Hartree-Fock equations describe motion of a particular electron in response to an averaged field due to the remaining electrons. The configuration interaction (CI) method is used to overcome this shortcoming. Here more than a single configuration is calculated simultaneously; the energy states are calculated in a variational manner. In constructing a DIM surface, separated energy states of the reactant and product molecules are brought together to form the complex energy states in much the same way molecular orbitals are calculated for a molecule from the atomic orbitals of the constituent atoms. Consequently the entrance and exit channels of a DIM surface can be very accurate, being fitted to very accurate spectroscopic or theoretical energy eigenvalues of the separated molecules. The interaction region may be fitted to ab initio points.

Using a more simplified theoretical approach, the dominating long range potential under which an ion-molecule pair interacts has the form

$$V(r) = -\frac{e^2\alpha}{2r^4}$$

where e is the charge of the ion, α is the electric polarizability of the neutral (without a permanent dipole moment), and r is the distance between the ion and molecule.[7] Given an initial relative velocity g, the impact parameter b_0 for which the ion-molecule pair will orbit each other is

$$b_0 = \left(\frac{4e^2\alpha}{\mu g^2} \right)^{1/4}$$

where μ is the reduced mass of the reactant system. Assuming all impact parameters $b<b_0$ lead to reaction, the reaction cross section (or Langevin cross section) has the form

$$\sigma(g) = \pi b_0^2 = \left(\frac{\pi}{g} \right) \left(\frac{4e^2\alpha}{\mu} \right)^{1/2}$$

The cross section is inversely proportional to the relative velocity and thus inversely proportional to $E^{1/2}$, the square root of the translational energy. The rate is calculated as the product of the cross section with velocity and is found to be energy (or temperature) independent. Many ion-molecule reactions have been found to proceed close to the Langevin rate which can be a rate larger than the gas kinetic collision rate.[8]

The ion-induced dipole potential is the long range force leading to the attractive well found at small internuclear distances between all the atoms involved on the ion-molecule PES. The well, a consequence of the chemical forces involved, can be quite substantial in some cases (a few eV deep) and generally extends quite far out due to

the r^{-4} term in the potential. Basically this well can influence the reaction in one of two ways. If the reactants can come together and tranfer some of their collision energy into internal degrees of freedom such that the complex will be captured in the well for more than a couple of rotational periods (about 10^{-13} sec), then products will separate isotropically without knowledge of initial conditions. Product intensity which is found symetrically about the ±90° scattering angle on center of mass (CM) velocity diagrams is indicative, but not conclusive of a long lived complex.

If the reaction does not proceed via a long lived complex, it is a direct reaction and is characterized by an assymmetry of product intensity about the ±90° scattering angle on CM velocity maps. If the kinetic energy is raised, eventually a long lived complex reaction will become direct because not enough internal degrees of freedom can be found in the collision complex in which to partition the reactants' energy to cause the complex to be quasibound within the well. Complex lifetimes may be estimated through the use of a variety of unimolecular reaction rate theories. In particular the statistical-mechanical Rice-Ramsperger-Kassel-Marcus (RRKM) theory has proven useful in predicting complex lifetimes provided the reaction does go through a long lived complex.[9] The complex lifetime is governed by the complex's total internal energy as compared to the minimum energy needed for decomposition and by the density of internal states over which the internal energy may be distributed. Non-fixed energy (energy not tied up in inactive internal modes) is assumed to be subject to rapid

statistical redistribution throughout the active vibrations and rotations of the complex. The lifetime decreases as the internal energy increases or as the molecular complexity decreases. The RRKM lifetime may be compared to the complex rotational period to predict the existence of a long lived complex or a direct reaction mechanism. Obviously a doubly differential cross section experiment is required to ascertain such dynamic information about the reaction.

In lieu of detailed theoretical calculations, simple models are often used to help elucidate the reaction dynamics. Mahan was quite successful in explaining reaction mechanisms through the use of electronic state correlation diagrams as crude PES's.[10,11] The ground and electronically excited states of reactants, products, and complexes for a variety of collision geometries are plotted relative to one another against an energy scale. The states are correlated to one another through spin correlation rules and symmetry properties. With this diagram one may trace reactants to products and see which complex states may play a role in the reactive scattering. Reactants sometimes may have access to the deep well of the reaction complex posing the possibility of the existence of a long lived complex, which can be investigated experimentally. Without benifit of a PES, however, many ion-molecule reactions can be described dynamically by such simple models as spectator stripping (SS),[12-14] knockout,[15] sequential impulse,[16,17] and long lived complexes[18,19] among others.

One interesting feature about ion-molecule reactions is that since quite often the ionization potentials (IP) of the neutrals A and B for

the reaction $[A + B]^+$ are close to one another, the two charge transfer (CT) states account for two low lying PES's which play important roles in the reaction dynamics. Because of the number of surfaces involved in the proximity of the reactants' total energy (due to different electronic states and collision geometries), the reactive scattering may proceed with the possibility of probing the potential well of the complex or the scattering may be direct in nature. The effect of multiple PES's was seen to be important in the CT and proton transfer (PT) reactions of H_2^+ with D_2, Ar, and N_2.[20-22] In these systems the IP of H_2 is close to that of the neutral reagent; the adiabatic PES has two entrance valleys (along the $[H_2\text{-}X]^+$ reaction coordinate) due to each CT state of the reactants. These valleys have an avoided crossing because they are states of the same symmetry. The reactants can easily move from one valley to another as the reaction progresses. This behavior is used to explain the trends seen in the total cross section as a function of both vibrational and translational energy. In particular for the ArH_2^+ system, at high collision energies (6-9 eV), the PT reaction cross section reflects the CT reaction. Both reaction channels exhibit very similar dependences of the reaction cross section on vibrational energy and this behavior strongly suggests that both reactions share a common portion of the PES.

In an effort to understand more about the dynamics of ion-molecule reactions, total cross section measurements are described in this thesis using the photoionization octapole guided ion technique. The PT reactions of H_2^+ and HD^+(v=0-4) with He and the H atom abstraction

of H_2 by $C_2H_2^+(v=0-2)$ are studied as a function of vibrational and translational energy. Vibrational state selection is accomplished by the photoionization technique. The use of the octapole ion guide ensures a high collection efficiency of all ions and therefore accurate relative total cross section measurements as a function of ion vibrational energy. The H_2^+ + He reaction was chosen because it is one of the simplest ion-molecule reactions (3 nuclei and 3 electrons) for which PES's may be calculated. Because the He ionization potential is so much higher than that of H_2 and because excited electronic states of H_2^+ are energetically inaccessable in the experiments described herein, this reaction is expected to take place on a single PES. In particular HD^+ was used as an isotopic aid in order to understand the H_2^+ + He reaction. $C_2H_2^+ + H_2$ was studied because very few greater than 3 atom endothermic reaction systems have been unambigiously studied comparing translational to vibrational energy competition in influencing the reaction cross section. This complex reaction is not well understood theoretically.

Both ground state reaction systems share similarities in that they are both endothermic reactions at thermal translational energy. For both systems vibrational energy may be put into the ion to energetically overcome the reaction endoergicity. At low collision energies, both systems are found to be strongly vibrationally enhanced even though the translational energy exceeds the reaction endoergicity. In the HeH_2^+ case, vibrational energy is put into the reaction coordinate itself to drive the proton transfer reaction. Simplistically, added

vibrational energy extends the H_2^+ bond and thereby helps to break it in order for proton tranfer to proceed. Looking at the other system, however, vibrational energy put into $C_2H_2^+$ to promote H_2 bond breakage to form $C_2H_3^+$ is not directly related to the reaction coordinate for this reaction. The role that vibrational energy plays in affecting the cross section is less well understood for such a reaction. These data complement and extend previous experimental and theoretical studies of these reactions.

References

1. E. W. McDaniel, V. Cermak, A. Dalgarno, E. E. Ferguson, and L. Friedman, Ion-Molecule Reactions, John Wiley and Sons, Inc., N. Y., 1970
2. J. L. Franklin, editor, Ion-Molecule Reactions, Plenum Press, N. Y., 1972
3. W. A. Chupka and M. E. Russell, J. Chem. Phys. 48, 1527 (1968)
4. H. S. W. Massey, E. H. S. Burhap, and H. B. Gilbody, Electronic and Ionic Impact Phenomena, Volume II, Electron Collisions with Molecules and Photoionization, Oxford University Press, London, 1969, pgs. 910, 972, 1145, and 1151
5. J. Berkowitz, Photoabsorption, Photoionization, and Photoelectron Spectroscopy, Academic Press, N. Y., 1979, pg. 213
6. R. B. Bernstein, editor, Atom-Molecule Collision Theory, A Guide for the Experimentalist, Plenum Press, N. Y., 1979
7. G. Gioumousis and D. P. Stevenson, J. Chem. Phys. 29, 294 (1958)
8. M. T. Bowers and D. D. Elleman, J. Chem. Phys. 51, 4606 (1969)
9. P. J. Robinson and K. A. Holbrook, Unimolecular Reactions, John Wiley and Sons, Inc., N. Y., 1972, chap. 4
10. B. H. Mahan, J. Chem. Phys. 55, 1436 (1971)
11. B. H. Mahan, Acct. Chem. Res. 8, 55 (1975)
12. A. Henglein, K. Lacmann, and G. Jacobs, Ber. Bunsenges. Phys. Chem. 69, 279 (1965)
13. K. Lacmann and A. Henglein, Ber. Bunsenges. Phys. Chem. 69, 286 (1965)

14. K. Lacmann and A. Henglein, Ber. Bunsenges. Phys. Chem. 69, 292 (1965)

15. J. C. Light and J. Horrocks, Proc. Phys. Soc. (London) 84, 527 (1964)

16. K. T. Gillen, B. H. Mahan, and J. S. Winn, J. Chem. Phys. 59, 6380 (1973)

17. B. H. Mahan, W. E. W. Ruska, and J. S. Winn, J. Chem. Phys. 65, 3888 (1976)

18. B. H. Mahan and T. M. Sloane, J. Chem. Phys. 59, 5661 (1973)

19. M. H. Chiang, E. A. Gislason, B. H. Mahan, C. W. Tsao, and A. S. Werner, J. Phys. Chem. 75, 1426 (1971)

20. S. L. Anderson, F. A. Houle, D. Gerlich, and Y. T. Lee, J. Chem. Phys. 75, 2153 (1981)

21. F. A. Houle, S. L. Anderson, D. Gerlich, T. Turner, and Y. T. Lee, J. Chem. Phys. 77, 748 (1982)

22. S. L. Anderson, T. Turner, B. H. Mahan, and Y. T. Lee, J. Chem. Phys. 77, 1842 (1982)

CHAPTER 2 EXPERIMENT

Total cross section measurements

Total integral cross sections were measured on the machine pictured schematically in Figure 2.1. Briefly, a beam of neutral molecules is photoionized with some selected wavelength (for which the vibrational population is well characterized) inside an RF octapole ion guide. The ions are formed into a beam, guided along the octapole axis, and are accelerated through a scattering cell surrounding a section of the octapole guide with a measured pressure of neutral reagent gas. Product ions are extracted from the octapole, mass analyzed, and counted.

We have studied both reactions of H_2^+ (or HD^+, v=0-4) and $C_2H_2^+$ (v=0-2). For the production of H_2^+, light from a 11 inch quartz capillary He pulsed discharge lamp is directed through a 180 micron entrance slit, two regions of differential pumping, onto a Bausch and Lomb 1200 lines/mm Os coated concave diffraction grating blazed at 800 Å. The grating is mounted in a McPherson 225 1 meter near-normal incidence monochromator. The diffracted wavelength of choice is then focussed through the 380 micron exit slit into the octapole ion source where it intersects a molecular beam of H_2. The beam source will be described in detail later.

This light source is described in more detail by Samson.[1] The He discharge produces a continuum centered about 810 Å and extending beyond 1000 Å. The power supply is usually run at a 60 KHz repetition rate with 40-50 torr He in the lamp.

H_2 photoionizes at a threshold of 803.2 Å (15.43 eV) predominently via an autoionization mechanism.[2] The light pumps H_2 up to vibrationally excited Rydberg states. Only the sum of the Rydberg energy with the vibrational energy, E_v, is above the ionizing threshold to produce $H_2^+(v')$. In H_2, autoionization occurs such that $\Delta v=1$ where energetically possible or it predominently leaves H_2^+ in its highest possible vibrational state.[3] Also there exists some smaller contribution of direct ionization to the H_2 ionization process which is governed primarily by Franck-Condon transitions. The relative populations of the H_2^+ vibrational levels at different ionizing wavelengths has previously estimated[4] and is shown in Table 2.1. H_2^+ cross sections are given in both its raw and vibrationally deconvoluted forms as noted.

The HD used in this experiment was produced by reacting $LiAlH_4$ with D_2O.[5] The HD purity was better than 95 percent. The ionization wavelengths for producing specific vibrational states of HD^+ were chosen based on spectroscopic knowledge of where the vibrational energies of HD^+ lie[6] and on the low resolution HD photoionization efficiency spectrum obtained with this experimental arrangement. The wavelengths for each vibrational state were taken on clusters of autoionizing peaks which are as far away from adjacent vibrational levels as possible. The high resolution HD autoionization spectrum has been measured recently by Dehmer and Chupka.[7]. The autoionization and direct ionization contributions were integrated where the autoionization peaks were assumed to leave HD^+ in its highest possible vibrational state. Franck-Condon factors obtained by Berkowitz and Spohr are used to provide an estimate of the vibrational contribution from

direct ionization.[8] The relative vibrational populations estimated by this method are found in Table 2.1. The following wavelengths were used: v=0, 797 Å; v=1, 782 Å; v=2, 772 Å; v=3, 763 Å; and v=4, 754 Å. All the HD^+ data is left in its raw form. Table 2.1 gives the estimated vibrational population distributions for both H_2^+ and HD^+.

The production of $C_2H_2^+$ ions is done in a similar manner to that of H_2^+. For C_2H_2 photoionization light from a 11 inch capillary (the same quartz tube) H_2 DC discharge lamp is directed through a larger 330 micron entrance slit, through the same monochrometer arrangement as above, and finally through a 508 micron exit slit located at the ion source. The light used is from the H_2 many-lined spectrum which runs from 1300 to 900 Å.[9] The lamp is operated with 2 torr H_2 at 1.4 kV and 1.0 ampere. A monochrometer calibration and resolution determination in this wavelength region was accomplished by looking at the Lyman beta line at 1025.722 Å. Figure 2.2 plots $C_2H_2^+$ ion intensity as a function of monochrometer wavelength in 1 Å increments. Since the entrance and exit slits were smaller for the H_2^+ experiments, the following resolution arguments set an upper limit for all the experiments described in this work. Figure 2.2 shows the Lyman Beta line to be approximately 3 Å FWHM. At 1088 Å the grating dispersion[10] is 288 Å/°. The 0.020 inch exit slit subtends 0.029 ° at a distance of 1 m from the grating allowing a bandpass of 8.4 Å or 4.2 Å FWHM (assuming a triangular slit function). The experimental observation and calculation are in reasonable agreement assuming the Lyman beta line is negligibly Doppler broadened.

At threshold C_2H_2 ionizes via a Franck-Condon (FC) process.[11] The threshold is located at 1088 Å (11.40 eV) and the ion yield exhibits step structure when the ν_2 C-C vibrational mode of the ion, the ⇐H⇐C-C⇒H⇒ symmetric stretch, is excited as ionizing wavelength is decreased. The relative step sizes for v=0:1:2 is 1.00:0.33:0.11 which is exactly the calculated relative FC factors for the transitions of C_2H_2 (v=0) to those vibrational states. Assuming the relative step heights represent the relative vibrational populations at a given wavelength, Table 2.2 is derived giving vibrational distributions for $C_2H_2^+$. The following wavelengths were used: v=0, 1076 Å; v=0 and 1, 1056 Å; and v=0, 1, and 2, 1034 Å. All ionizing wavelengths leave the $C_2H_2^+$ molecule predominantly in the v=0 state.

The ion beam source is basically the same as that described previously.[4] The neutral beam is formed into a supersonic beam, collimated, and introduced into the ionization chamber. There the beam intersects the focussed, monochromatic light in a volume roughly 1.3 mm in diameter by 1 cm in length.

The H_2^+ and HD^+ experiments were done with an improved neutral source; a 30 micron nozzle was placed 0.819 inches from a 0.016 inch diameter electroformed skimmer tip. The skimmer tip to the end of the octapole ionization source was 2.115 inches. The nozzle pressure for H_2 was set at 80 psi producing roughly 15 KHz v=0 H_2^+ ions and HD was run at 70 psi to yield 12 KHz HD^+ in v=2. A more detailed explanation of the improvements of this source over earlier experiments on this machine is given in the H_2^+ + He chapter.

The $C_2H_2^+$ experiments were run with a 70 micron nozzle placed 0.778 inches from the same skimmer. All other beam source dimensions were kept the same. The C_2H_2 was run through a dry ice-ethanol trap (to remove acetone) and pressurized behind the nozzle to 400 torr. Under these conditions the $C_2H_2^+$ ion count rate was approximately 1 KHz for v=2.

The molecular beam and light beam intersect inside an RF octapole ion guide. The ion guide consists of (8) 1/8 inch molybdenum rods symmetrically spaced around the circumference of an imaginary 1 inch diameter cylinder. Alternate rods are connected to opposite phases of a 15 MHz tunable RF generator. The effective potential inside the ion guide is described by the equation

$$V_{eff} = \frac{e^2 V_0^{rf}}{4mw^2 R_0^2} \left(\frac{R}{R_0} \right)^6$$

where V_0^{rf} is the peak RF voltage, R_0 is the radius of the cylindrically placed rods, R is the radial distance if the ion from the octapole axis, w is the RF frequency, and m is the ion mass.[12]

The octapole is broken into four segments (J_i) to which separate DC potentials are applied as shown in Figure 2.2. This allows control of ion translational energy. The segments are capacitively coupled in series from the driven octapole (the ion source). A scattering cell surrounds a length of the last octapole and is filled with some measured pressure of a neutral reagent gas. All ion-molecule reactions

occur within the octapole; use of the octapole ensures 100 percent transmission and collection efficiency of all product ions.

Product ions (or reactant ions) are extracted from the octapole by a set of conventional ion optics, accelerated to 70-90 eV for mass analysis by a quadrupole mass spectrometer, and are counted by the detector. The scintillator and PMT of the original Daly detector was replaced by a solid state Li drifted Si detector. Ions are accelerated to an electrode of -33 kV potential from which secondary electrons are ejected. The number of secondary electrons, n, ejected per incident ion has a Poisson probability which is dependent on the ion mass and impact energy and can be written as

$$P_n = \frac{e^{-\alpha}\alpha n}{n!}$$

where α is the average number of electrons ejected in the pulse.[13,14] The electrons are accelerated across the -33 kV potential to the face of the liquid N_2 cooled Li drifted Si detector biased 900 V below ground potential. The voltage across the detector itself is 900 V to ground. This solid state detector is used to count bursts of electrons produced per ion to accomplish single ion detection.

The great advantage that this solid state detector has over the usual Daly detector is its substantially better energy resolution, that is its ability to resolve the number of electrons contained in each signal pulse. Because the scintillation and photoemission mechanism is relatively energy inefficient, large statistical flucuations

in the pulse heights result from the pulse of electrons striking the scintillator. Only about 3 eV is required to produce a hole-electron pair in a Si detector; this energy is about 100 times smaller than that for scintillation detectors.[15] Consequently statistical flucuations in the charge production process are greatly reduced and resolution is improved.

When the secondary electrons impact upon the detector, electron-hole pairs are formed which are swept out by the 900 V bias voltage. This charge triggers an FET located directly behind the Si wafer itself and serves as the first preamplifier stage; the entire preamplifier is located as close to the detector as possible. The preamplifier also includes a test pulse input. The amplified pulse is then fed into a pileup rejecter. The pileup rejecter is an integral unit containing an amplifier, pileup rejecter (to keep pulses from piling up if the signal rate is too high), and discriminator. The output of the pileup rejecter is a logic pulse suitable for scalar counting.

Figure 2.3 shows the pulse height distribution of secondary electron emission of -33 kV H_2^+ ions impacting the electrode. One can see that at this energy, H_2^+ most probably causes the ejection of 4-5 electrons from the electrode surface. Because the detector has such high resolution, one can accurately set the discriminator to avoid counting n, n-1, n-2, ... electron events. The major noise in the entire detector system is field emission from the high potential electrode which are 1 electron events. Accurately setting the discriminator obviously wastes the least signal counts especially in low cross

section reactions as described in this thesis. For H_2^+, the n=1 peak constitutes less than 3 percent of the total H_2^+ signal. Figure 2.3 also shows the pulse height distribution avoiding the n=1 electron events; the discriminator is set at 8.18. The discriminator is set at 8.60 for discriminating n=2 electron events. Increasing the ion mass or energy will cause a higher yield of secondary electron emission.

Signal plus background counts are taken with the scattering cell filled with reagent gas (S+B) and with the cell off to count background (B). The cross section is calculated as

$$\sigma = \frac{(S+B)-B}{Inl}$$

where I is the unattenuated primary ion beam intensity, n is the number density of the neutral gas known by Baratron capacitance monometer absolute pressure measurement, and l is the effective scattering cell length.

The experiment may be run in two different modes. The collision energy may be fixed and the wavelength (or vibrational states) may be scanned. Or the photoionizing wavelength is fixed and signal is taken as a function of collision energy. Usually for data analysis a best energy scan is taken as the standard to which all the wavelength scans at the varios energies are normalized. Doing both wavelength and energy scans provides an internal check to the cross sections; one normalizes all the data to one vibrational level at one energy. Typically the wavelength and energy scans agree to within 20 percent (as in the HeH_2^+ experiments where the cross section is less than 2.5 $Å^2$).

The error is hard to estimate, however the absolute cross sectional error is estimated to be less than 25 percent while the relative error between vibrational states is estimated to average less than 10 percent.

The raw cross sections are vibrationally deconvoluted once they are calculated and normalized. The vibrational population distributions for H_2^+, HD^+, and $C_2H_2^+$ are given in Tables 2.1 and 2.2. Because at each wavelength the H_2^+ and HD^+ ions are expected to be fairly vibrationally pure, the cross sectional trends seen in the raw data are merely enhanced in the deconvoluted data. However for $C_2H_2^+$, since at each wavelength the vibrational distribution is largely v=0, the deconvolution process may introduce vastly differing cross sectional variation versus vibration for similar sets of raw data. Repetitive experiments were run in an effort to overcome this problem. In any case both the raw and vibrationally deconvoluted cross sections are tabulated.

References

1. James A. R. Samson, Techniques of Vacuum Ultraviolet Spectroscopy, Pied Publications, Lincoln 1967, page 101
2. P. M. Dehmer and W. A. Chupka, J. Chem. Phys., 65, 2243 (1976)
3. J. Berkowitz and W. A. Chupka, J. Chem. Phys., 51, 2341 (1969)
4. Scott L. Anderson, F. A. Houle, D. Gerlich, Y. T. Lee, J. Chem. Phys.,75, 2153 (1981)
5. I. Wender, R. A. Friedel, and M. Orchin, J. Am. Chem. Soc. 71, 1140 (1949)
6. K. P. Huber and G. Herzberg, Molecular Spectra and Molecular Structure IV. Constants of Diatomic Molecules, Van Nostrand Reinhold Co., N. Y. 1979, page 272
7. P. M. Dehmer and W. A. Chupka, J. Chem. Phys., 79, 1569 (1983)
8. J. Berkowitz and R. Spohr, J. Electron. Spectrosc. Relat. Phenom., 2, 143 (1973)
9. See reference 1, page 139
10. Bausch and Lomb, Diffraction Grating Handbook, 1970, pages 16-20
11. Vernon H. Dibeler and James A. Walker, Int. J. Mass Spec. Ion Phys., 11, 49 (1973)
12. S. W. Bustamente, Ph.D. thesis, University of California, Berkeley, pgs. 40, 41
13. L. A. Dietz, Rev. Sci. Inst. 36, 1763 (1965)
14. H. M. Gibbs and E. D. Commins, Rev. Sci. Inst. 37, 1385 (1966)
15. F. S. Goulding, Nuc. Inst. Methods 43,1 (1966)

Figure captions

FIG. 2.1. Machine schematic. J_i are the seperately biased octapole segments. XBL 808-10865A

FIG. 2.2. $C_2H_2^+$ ion intensity versus monochrometer wavelength in 1 Å increments. XBL 842-737

FIG. 2.3. Pulse height distribution of secondary electron emission from 33 KeV H_2^+, with the discriminator set at 8.18 to cut out n=1 electron events on the left and no discrimination pictured on the right. Peak is at n=4. XBB 842-1230

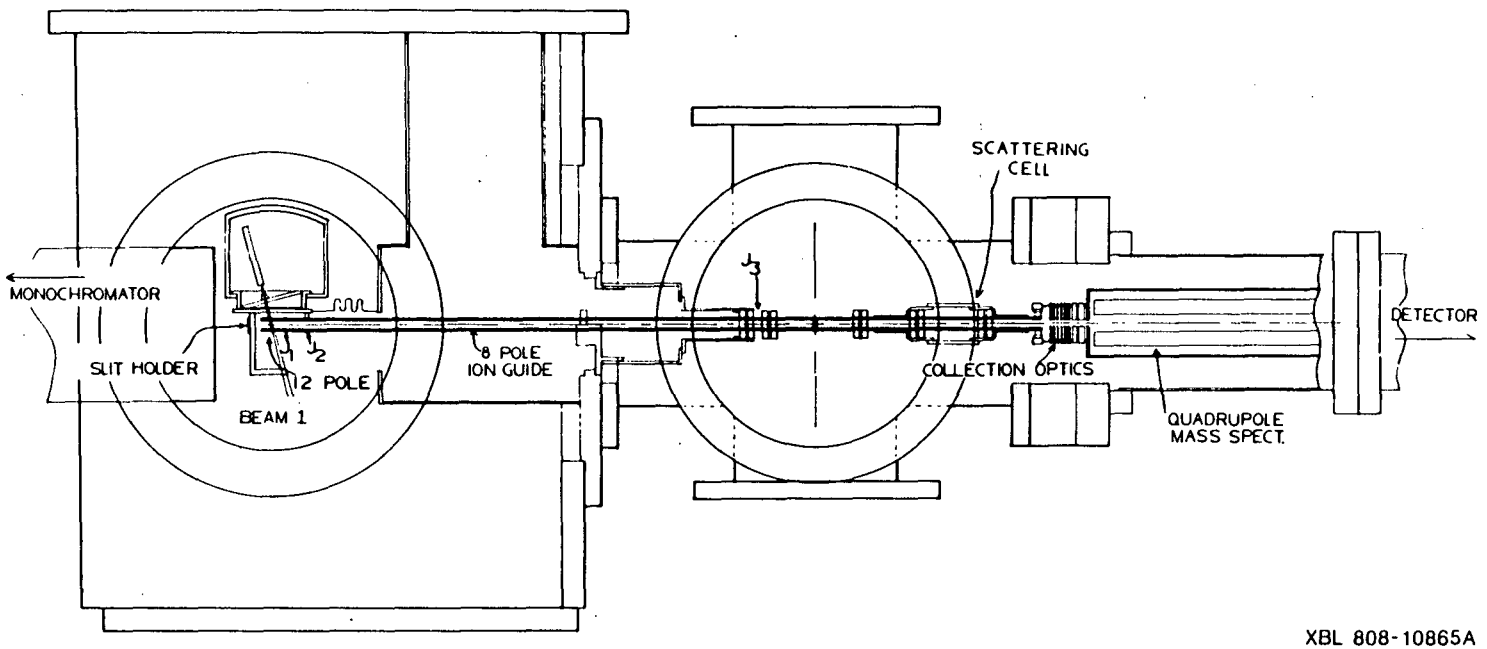
MONOCHROMATOR
SLIT HOLDER
BEAM 1
2 POLE
8 POLE
ION GUIDE
SCATTERING
CELL
COLLECTION OPTICS
QUADRUPOLE
MASS SPECT.
DETECTOR
XBL 808-10865A

Fig. 2.1

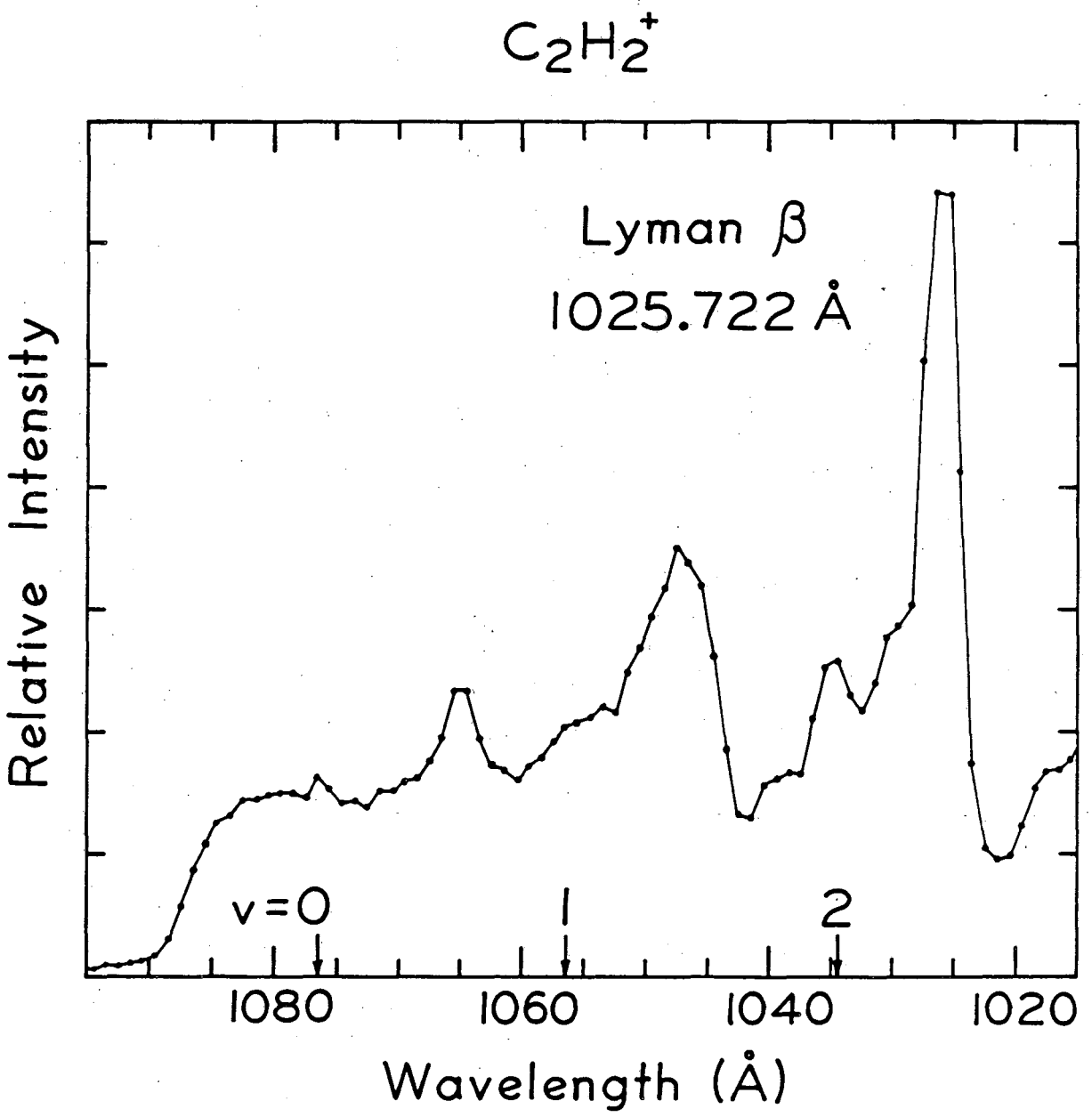

XBL 842-737

Fig. 2.2

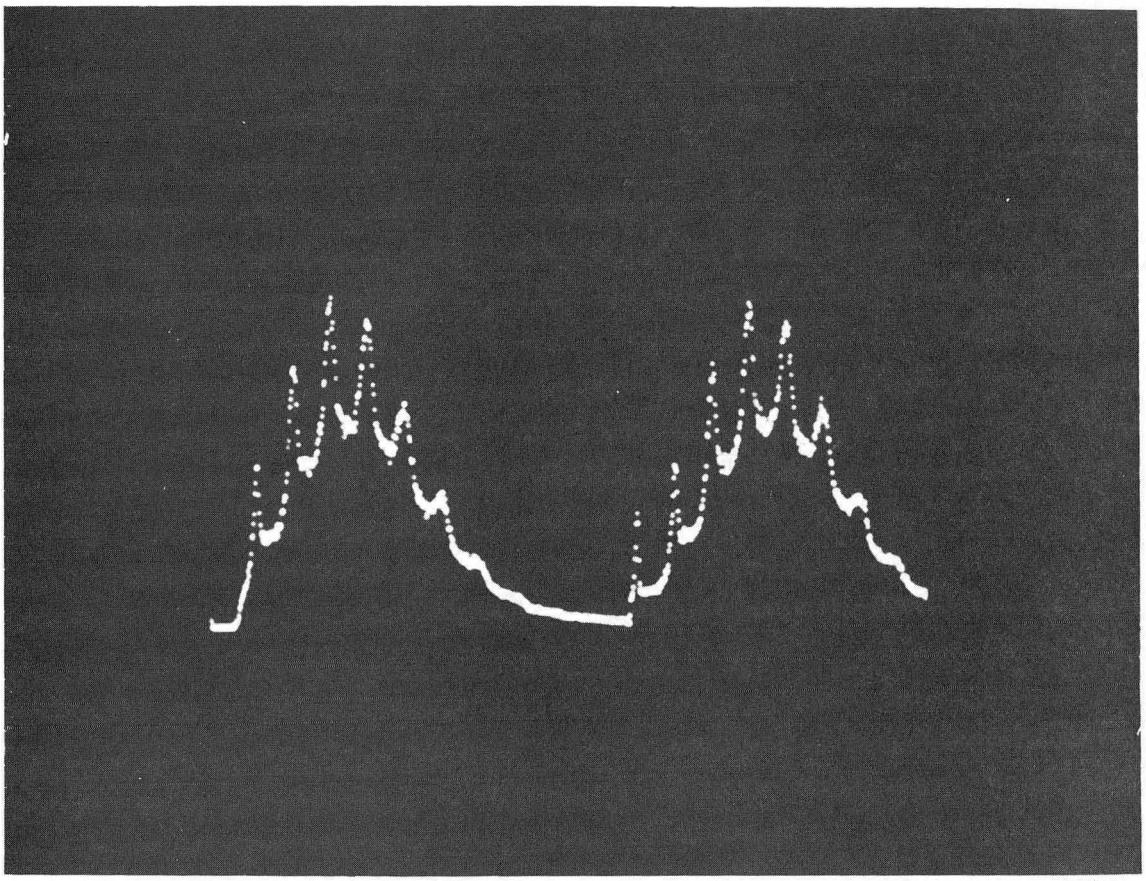

XBB 842-1230

Fig. 2.3

Tables

TABLE 2.1. Estimated vibrational state distributions for H_2^+ and HD^+.

Estimated vibrational distribution	H_2^+ v nominal 0	1	2	3	4	HD^+ v nominal 0	1	2	3	4
0	1.000	0.107	0.078	0.085	0.070	1.000	0.139	0.108	0.083	0.077
1		0.893	0.161	0.174	0.145		0.861	0.220	0.168	0.156
2			0.761	0.188	0.157			0.672	0.206	0.191
3				0.553	0.152				0.543	0.184
4					0.476					0.392

TABLE 2.2. Estimated vibrational distributions for $C_2H_2^+$.

actual vibrational distribution	v nominal 0	1	2
0	1.000	0.752	0.694
1		0.248	0.229
2			0.076

CHAPTER 3 H_2^+, HD^+ + He

Introduction

The reaction between H_2^+ and He forming HeH^+ has been extensively investigated in the past. This reaction is endothermic by 0.8 eV and was the first experimental example, as shown by Chupka, et. al., that vibrational energy strongly promotes product formation over kinetic energy.[1,2] Aside from these photoionization studies which prepared H_2^+ in a specific vibrational state, most past experimental work, including crossed beam,[3-5] mass spectrometric,[6,7] merged beam,[8] and ion beam-gas cell[9] techniques, used H_2^+ produced by electron impact ionization of H_2; thus a broad range of H_2^+ vibrational states participated in the reaction with He. These studies all give evidence to a direct reaction with a maximum cross section for HeH^+ production of approximately 5 $Å^2$ at a collision energy of 1 eV in the center of mass (CM) coordinate system. The cross section decreases sharply with the increase of collision energy beyond 1 eV. The crossed beams studies of Herman, et. al.[4,5] have shown the reaction to proceed mainly via the spectator stripping (SS) mechanism when the collision energy is between 0.5 and 4.0 eV. However, when H_2^+ was specially prepared to be in lower vibrational states, the intensity of products which can be ascribed to the SS mechanism is substantially smaller.

This system is one of the simplest ion-molecule reactions for which potential energy surfaces can be rigorously calculated. Because of the large difference between the ionization potentials of He and

H_2, the excited and charge transfered states of this triatomic system lie appreciably above the ground state[10,11] and the reaction between H_2^+ and He, at low collision energies, is expected to take place on a single potential energy surface. Brown and Hayes have calculated an ab initio surface for the linear $H_2^+ + He \rightarrow HeH^+ + H$ reaction.[12] Their surface shows a barrier late in the exit channel and the existence of a small well (0.15 eV below reactants) cooresponding to a weak HeH_2^+ complex. The linear complex has been shown to be the most stable geometry. Kuntz then fit this surface to a surface generated by the diatomics-in-molecules (DIM) method;[13] however, quantum mechanical (QM) scattering calculations using this surface does not give the experimentally observed enhancement in the reaction cross section with an increase of H_2^+ vibrational energy.[14,15] The reaction probability as a function of collision energy shows sharp resonance structure above the reaction threshold with resonance widths ranging anywhere from 0.002 to 0.04 eV. The qualitative disagreement between experimental and calculated results may not be entirely due to the limitation of using the 1D collinear potential energy surface. Kuntz and Whitton have run classical trajectories on a revised DIM surface with good, qualitative experimental agreement.[16,17] Raff and his coworkers have also generated a spline fitted ab initio (SAI) surface which gives vibrational enhancement to the reaction probability in a collinear calculation using both QM and quasiclassical trajectory (QCT) methods.[18] They have also found that the difference in the shape of the inner repulsive wall between the SAI and DIM surfaces accounts for their

dynamical differences,[19] whereas including or excluding the potential well on a spline fitted DIM surface was shown by Sathyamurthy to have little effect.[20]

More recently McLaughlin and Thompson have calculated the four lowest electronic energies for HeH_2^+ in C_s symmetry; 596 ab initio points are reported for a total of 7 different bond angles.[21] Trajectory studies of both Hartree-Fock (HF) and the configuration interaction (CI) collinear versions of the surface give vibrational enhancement for reaction from v=0 to v=1, but the more accurate CI surface gives a decreasing reaction probability as vibration is increased.[22]

Although collinear QM scattering calculations on the original Kuntz DIM surface does not give the desired vibrational dependence, the three dimensional QCT results of Schneider, et. al.[23] were in satisfactory agreement with their experimental differential cross sections,[4,5] and, except for low translational energies and low vibrational states, they are in good agreement with the data of Chupka, et. al.[1,2]

Truhlar, et. al. extended the earlier application by Light and Lin[24] of statistical phase space theory to the H_2^+ + He reaction using an ion-induced dipole potential.[25,26] Although vibrational enhancement of the reaction is obtained, the cross section varies too slowly with energy, being too large for low vibrational levels and too small for higher levels. Apparently the full statistical assumption is not valid for this system.

In this chapter results obtained using our unique apparatus consisting of a photoionization ion source and octapole RF ion guide for the investigation of the reactions of $H_2^+(v)$ + He and $HD^+(v)$ + He are described. The 0-10 eV center of mass kinetic energy range used here extends as well as improves the knowledge of the translational energy dependence derived from previous photoionization studies. The previous studies of the translational energy dependence were derived from the repeller voltage dependence of the reaction taking place in the ion source. The substantially better kinetic energy definition between reactants in this experiment allows the direct determination of the microscopic cross section as a function of kinetic energies. New information on the HD^+ system, especially its cross section and branching ratio as a function of vibrational and kinetic energy of reaction provides additional information on the dynamical aspects of this reaction.

Part of the original motivation for carrying out the detailed investigation of the translational energy dependence of the reaction cross section for various vibrational states of H_2^+ was the possibility of experimentally observing the sharp resonances shown in the collinear QM calculations of the reaction probability as a function of collision energy.[14,15] No evidence of these resonances was detected in this experiment.

Results and analysis

H_2^+ + He

Figure 3.1 shows the raw data of the collision energy dependence of the reaction cross section for HeH^+ formation from state selected H_2^+. The wavelengths were chosen to produce the various $H_2^+(v)$ states shown. In all the cases except for v=0, the cross section rises sharply below 1eV (all kinetic energies are CM kinetic energies unless otherwise specified), peaks at 1-2 eV, then decreases sharply until about 4 eV. At 4 eV and above, the cross section decreases at a visibly slower rate. For the v=0 state, the cross section rises much more slowly, peaks broadly with a value of about 0.15 $Å^2$ around 3 eV, and decreases very slowly thereafter. Although the state selection is not pure, contamination of lower vibrational states for the chosen state tend to deemphasize the vibrational dependence, yet the vibrational enhancement of the cross sections can be clearly seen in these raw data. Figure 3.2 gives the cross section, deconvoluted for the vibrational state distribution of H_2^+, as a function of ion vibrational energy for a given kinetic energy. The reaction is substantially vibrationally enhanced at the lower translational energies. At 1 eV, the reaction probability is increased well over an order of magnitude for v=0 to 4, from 0.0569 to 1.67 $Å^2$. At 2 eV, near the cross section maximum, the cross section varies from 0.129 to 0.964 $Å^2$ for v=0 to 4. Above 5 eV, little vibrational dependence is seen. Table II gives the values of the cross section as a function of kinetic and vibrational energy for both the raw data and the deconvoluted results.

$HD^+ + He$

Figure 3.3 shows raw data plots of HeD^+ production as a function of kinetic energy. The reaction is again strongly vibrationally enhanced at low kinetic energy and the cross section at maximum is roughly the same as that for HeH^+ production from H_2^+. Owing to the limited supply of HD available, only one extensive energy scan of the HeH^+ channel was made and is shown in Figure 3.4. The cross section drops more sharply with collision energy than for the HeD^+ channel. An improved ion source was required because the ion-molecule reaction of HD^+ with itself in the ion source interferes with the same mass product of HeH^+ we were trying to detect. A new electroformed skimmer and an increased nozzle-skimmer distance were used in the experiment in an effort to clean up the supersonic HD beam in the ion source. A cleaner HD beam produced less background HD gas with which the HD^+ could react. Data shown in Figure 3.4 are the results using the improved source, which substantially decreased the time needed to obtain the HeH^+ signal with reasonable statistical errors. The HeH^+ channel cross sections were normalized to the data found in Figure 3.4. Figure 3.5 shows the $HD^+(v=4)$ to the same product cross section similar to Figure 3.4. This scan was made with 3/4 counting time and 1/2 the ion beam intensity as that of Figure 3.4. Obviously the statistics of Figure 3.5 are too poor to be useful for normalizing the wavelength scans.

Figure 3.6 shows the dependence of the reaction cross section on HD^+ vibration at various kinetic energies for both the HeH^+ and HeD^+

channels. These data are deconvoluted from the raw data based on the estimated HD^+ vibrational state distributions given in Table 2.1. For HeH^+ formation at 1 eV, the reaction is strongly vibrationally enhanced, increasing one order of magnitude for v=0 to 4, from 0.099 to 2.25 $Å^2$. Vibrational enhancement is seen up to 4 eV. By 8 eV, the cross section shows only a slight vibrational enhancement. In contrast the HeD^+ channel shows little vibrational dependence at 4 eV even though at 1-2 eV both channels behave similarly. By 8 eV, the HeD^+ channel shows a noticeable vibrational inhibition. The branching ratio for the formation of HeH^+ to HeD^+ is 1.79:1 for HD^+(v=4) at 1 eV. Table III gives the values of the cross sections for both reaction channels as a function of kinetic and vibrational energy for both the raw and deconvoluted data.

Discussion

Herman, et. al. have studied the reaction of H_2^+, formed by electron impact, with He in the 0.5-4.0 eV range using the crossed beams method and have found most of the product HeH^+ peaked at spectator stripping (SS) velocities.[4] The data presented here indeed contain some features which support the significant involvement of the SS mechanism for this reaction when H_2^+ is vibrationally excited.

The role played by the SS mechanism can be seen in Figure 3.1. For v=1-4, above 3 eV, the cross section decreases rapidly for vibrationally excited H_2^+, but around 4 eV the rate of decrease becomes markedly slower as if a sudden disappearence of a reaction mechanism occurs leaving a second reaction mechanism which does not strongly depend on collision energy. The range of collision energies in which the breaks in the cross sections occur for various H_2^+ vibrational states is exactly the range of critical energies for the SS mechanism.

The range of kinetic energies over which product formation by SS is stable is calculated in a straightforward manner. In the CM frame, the SS model implies that the He atom abstracts the proton without imparting any momentum to the remaining H atom of the original H_2^+ molecule. If HeH^+ is to be formed, the two body kinetic energy between He and H^+ must be larger than the reaction endothermicity, but no more than the binding energy of H_2^+. Below the threshold energy, the product formation is energetically impossible and above the critical energy, HeH^+ formed will contain too much internal energy to be

bound. Table IV lists the kinetic energy range for each ion vibrational level for which SS is stable. The energy range for the formation of stable products via the SS model shifts for each vibrational level of H_2^+ by that vibrational energy in the 2 body (H^+ + He) CM frame. The 3 body (H_2^+ + He) CM kinetic energy

$$E_{cm} = \frac{m_{He} \; m_{H_2^+} \; v_{rel}^2}{2m_{He+H_2^+}}$$

is related to the 2 body CM kinetic energy

$$E_{He,H^+} = \frac{m_{He} \; m_{H^+} \; v_{rel}^2}{2m_{He+H^+}}$$

by a factor of

$$\frac{m_{He+H^+} \; m_{H_2^+}}{m_{He+H_2^+} \; m_{H^+}} = \frac{5}{3}$$

that is

$$E_{cm}=(5/3)E_{He,H^+}.$$

Vibrational energy dependence of the reaction cross sections at various collision energies shown in Figure 3.2 also reveal the important role played by the SS mechanism. For example at 4 eV the cross section decreases from v=2-4. Referring to Table IV reveals that HeH^+

cannot be formed via a SS mechanism for these vibrational levels at this collision energy. At 8 eV, the strong vibrational enhancement is completely absent and energetically product cannot be formed by SS. The breaks in the collision energy dependence of the reaction cross section shown in Figure 3.1 are dependent on the vibrational state of H_2^+. For v=3, this break occurs at 3.4 eV, close to the calculated critical energy for SS. For v=2, the break moves up with energy to 4 eV as expected. The fact that a visible break does occur near the SS critical energy supports the presence of the SS mechanism for this reaction.

The role played by the SS reactions is seen to become more and more important as the vibrational energy in H_2^+ is increased. For v=0, the cross sectional dependence as a function of kinetic energy shows a broad peak which decays slowly with energy. Here one must assume that SS does not play as important a role as in the case of vibrationally excited H_2^+. The small magnitude of the cross section (under 0.15 $Å^2$) and the slow variation of the cross section with kinetic energy indicate that this v=0 reaction probably proceeds mostly via intimate, small impact parameter collisions which involve all three atoms. The increase of vibrational energy not only reduces the dissociation energy, but also extends the average H_2^+ bond distance which facilitates the capture of H^+ in H_2^+ by He as a two body collision, leaving the H atom as a spectator. Pacak, et. al. have looked at HeH^+ formation using a v=0,1 enhanced H_2^+ beam.[5] The contour maps of product angular and velocity distributions at 3.58 eV

reveals a substantial amount of product which is backscattered with respect to the He direction; this backscattered peak is approximately 2/3 the intensity of the forward peaked product. Using a nonselected H_2^+ beam (produced by electron bombardment ionization) at a similar collision energy, the forward peak is 5 times the backscattered peak,[4] that is, H_2^+ in higher vibrational levels reacts to form product mainly in the forward direction.

Above the critical energy for the SS mechanism, the formation of HeH^+ is only possible when the H atom ceases to be a spectator and the extra energy is carried away as the relative motion between the H atom and HeH^+ molecule. The reaction mechanism must remain direct and is most likely a sequential impulse type of mechanism[17,27] which forms the product at predominently small impact parameters. Energetically the collision induced dissociation (CID) channel opens up at the bond energy of H_2^+, 2.65 eV. But, for vibrationally excited H_2^+, CID only becomes important beyond the critical energy for the SS mechanism. Chupka, et. al. have indeed found CID to be vibrationally enhanced.[2] Their data shows that for v=0 the cross section is small, comparable to that of proton transfer and for v=3 the cross section rises slowly and peaks at 6 eV total energy. All these results indicate a clear relation between SS and CID at collision energies beyond the critical energy of the SS mechanism; at translational energies above 4 eV, vibrational inhibition exists as a result of CID competition against proton transfer. The trajectory studies of Whitton and Kuntz also indicate that CID is vibrationally enhanced.[17]

The CID mechanism using SS as an intermediate step can be viewed in two ways. Either the H atom or the proton may be left after the reaction as the spectator. With the proton as the spectator, its velocity would simply be the same as the initial H_2^+ velocity. The He atom strips the H atom from the H_2^+ molecule leaving behind the proton to be detected in the direction of initial H_2^+ velocity. Havemann, et. al. do find a peaking of proton intensity occuring in the direction of the original H_2^+ motion close to the initial H_2^+ velocity.[28] If the H atom is the spectator, the He atom will strip the proton from the H_2^+ molecule to form HeH^+ which subsequently falls apart. H^+ is detected in the direction of the initial He atom (backward with respect to the initial H_2^+ motion). Because of the experimental difficulty in detecting these low laboratory energy, backward scattered protons in crossed beams experiments, the failure to observe backward scattered H^+ in the CID work of Havemann, et. al. might not imply a preference of H^+ to be the spectator over H in the CID of H_2^+ with He.

The qualitative agreement between this work and that of Chupka is satisfying. The proton transfer reaction for v=0 is in qualitative agreement, but for v=3 our cross sectional dependence differs somewhat from that of Chupka. Their data is found to peak sharply at 0.2 eV with a cross section of 5.2 $Å^2$ and it falls off sharply afterwards. In our data shown in Figure 3.1, the cross section rises sharply, but peaks at 1.7 eV with a value of 1.16 $Å^2$. After peaking the cross section also falls off sharply through 4 eV. The discrepencies in magnitude and where the maximum occurs may be due in part to the

experimental method.[1] In these pioneering studies of Chupka, et. al., the reaction took place in a single photoionization chamber where the ion kinetic energy was varied by changing the repeller voltage and a mass spectrometer sampled products from that chamber. Due to the presence of the electric field over which the H_2 molecules were photoionized and reacted, the ions reacted with He over a range of kinetic energies. Consequently, phenomenological cross sections were measured; microscopic cross sections were derived by use of a deconvolution method given by Light.[29] In the present experiment, the kinetic energy between H_2^+ and He is very well defined and the microscopic cross sections are measured directly.

Using HD^+ as the reactant ion, it is possible to verify many dynamical features of the HeH_2^+ system in greater detail. Both channels forming HeH^+ and HeD^+ exhibit the same qualitative features as for HeH^+ formation from H_2^+. At lower kinetic energy strong vibrational enhancement is seen which turns into vibrational inhibition as the collision energy is raised. The SS mechanism can again explain the cross sectional behavior. Here, $E_{cm}=(15/7)E_{He,H^+}$ for HeH^+ and $E_{cm}=(9/7)E_{He,D^+}$ for HeD^+ as SS formed products. As seen on Figures 3.3 and 3.4, the cross sections decrease similarly with collision energy over the energy range studied. The plot, however, does not show a sudden shift in this rate of decay as in Figure 3.1 for the HeH_2^+ system. Near 1 eV, the maximum cross section is 0.66 and 0.51 $Å^2$ for HeH^+ and HeD^+ respectively from HD^+, v=2 compared to 0.74 $Å^2$ for HeH^+ from H_2^+, v=2.

Different kinematic relations may be seen between the proton and deuteron transfer channels HeH^+ and HeD^+. Both channels exhibit similar vibrational enhancement at 1 and 2 eV. However, at 8 eV, the HeH^+ channel is slightly vibrationally enhanced for v=0-3 while HeD^+ is vibrationally inhibited for the same vibrational levels. The energy range for HeD^+ formation by the SS mechanism is lower than for HeH^+ as shown in Table IV. As the collision energy is raised, SS is closed to stable HeD^+ formation first. At 4 eV all vibrational levels except v=4 are open to SS for HeH^+, but no $HD^+(v)$ levels are open for HeD^+ SS formation. SS also manifests itself near its threshold at 1 eV. The cross section increases at an even rate of roughly 0.3 $Å^2$ with each vibrational level v=1-4 for the HeD^+ channel. All these vibrational levels are open to SS. But for HeH^+, only v=2-4 is accessible via SS. The v=0-1 increase is only 0.15 $Å^2$ while those for v=1-4 are each on the order of 0.4 $Å^2$ or greater. The larger cross section jumps correlate with the onset of SS channels.

The HeH^+:HeD^+ branching ratio is 1.79:1 for the reaction of $HD^+(v=4)$ with He at 1 eV relative translational energy. The cross section for $HD^+(v=2) + He \rightarrow HeH^+ + D$ shown in Figure 3.4 drops considerably faster than for $HD^+(v=2) + He \rightarrow HeD^+ + H$ in Figure 3.3. Possible charge induced orientation effects where the H atom points more towards the He atom during collision may account for a sharper rise of cross section at lower collision energies. At low energies a charge induced dipole interaction between HD^+ and He will govern the reaction dynamics of vibrationally excited HD^+. For HD^+ the charge is

centered between the two atoms and is shifted from the CM, which lies closer to the D atom. The charge induced dipole interaction, being much larger than the HD^+ rotational energy, may rotate the HD^+ about its CM preferentially pointing the positive charge and therefore the H atom towards the He atom. The He atom then abstracts the H^+ leaving the neutral D atom behind. Therefore the HeH^+ cross section would be enhanced over HeD^+. At higher energies when the charge induced dipole interaction becomes less important, the induced orientation effect disappears and the expected sharp cross sectional drop off can be seen as in Figure 3.4.

The potential energy surface for the HeH_2^+ system has its barrier, which is approximately the reaction endothermicity, late in its exit channel. Based on this feature, one may expect that vibrational rather than translational energy is more efficient towards making the proton transfer reaction proceed.[30] At low kinetic energies above the reaction threshold, this enhancement is indeed seen. Trajectory calculations using the DIM surface generated by Whitton and Kuntz have clearly demonstrated the reaction to be strongly vibrationally enhanced.[17] Potential energy contours of extended $H_2^+(v)$ molecules with respect to an incoming He atom show an attractive well which lies further from the center of H_2^+ (or is localized on one H atom) as v is increased. This effect becomes important from v=3-5 and illustrates how HeH^+ is forming as the H_2^+ bond is partially broken.

Their trajectory studies show good agreement with the present experiment. The v=0 total cross sectional dependence rises slowly,

peaks at 3 eV total energy (almost 0.5 $Å^2$), and then decays slowly in similar fashion to these results. The maxima for v=2 and v=3 are found at 1.3 and 1.4 eV respectively compared to 1.6 and 1.7 eV in this experiment. Also in agreement is v=3,4 where the cross sections decline rapidly until 4 eV where all the cross sections (v=0-4) decrease slowly and little vibrational dependence is seen in the cross section as function of total energy thereafter. In comparison with the results of our experiments, three major differences are noted: a) the v=0-1 enhancement is absent with v=1 nearly identical to v=0, b) v=2 does not rise and fall as steeply as it should, c) the magnitude of the total cross section is roughly a factor of 2 too large. They attribute the drop in reactive cross section at high translational energy (2-5 eV) to two reasons: a) as translational energy is increased, the maximum impact parameter decreases for which capture of He by H_2^+ is possible and b) compared to the ion vibrational period, as translational energy is increased, collision time becomes too short to allow the rearrangement to proceed.

In the same work Whitton and Kuntz have also calculated approximate 3D reactive cross sections for HD^+ + He. Both channels show strong vibrational enhancement. The v=3 HeD^+ curve falls too slowly and the cross sections are again too large, but the agreement is qualitatively assuring. The discrepencies between their calculations and this work may be due to their use of collinear points to generate 3D surfaces.

Classical trajectory calculations on some of the potential energy surfaces have reproduced many of the important features of this

reaction. A 3D quantum scattering calculation on a more accurate ab initio potential energy surface would be very useful for a better theoretical understanding of many of the fine details of the reaction dynamics.

The failure to observe resonances in the energy dependence of the total reaction cross section is not entirely surprising. Redmon and Wyatt have shown that for the 3D quantum calculations of $F + H_2$ reactions, since the reactants with different orbital angular momenta form quasibound states at different translational energies, the sharp resonances observed in the collinear quantum mechanical calculation of the energy dependence of reaction probability is likely to be smoothed out in a 3D reactive scattering calculation, especially when a substantial number of partial waves are involved in the scattering.[31] The experimental observation of reactive resonances for this system might only be possible with the measurement of vibrational state resolved product angular distributions at appropriate collision energies.[32]

Conclusion

In summary, total cross sections for the proton transfer reactions of H_2^+, HD^+ + He have been measured as a function of ion vibrational and collisional energy. The data are in qualitative agreement with previous work in the energy range where comparison can be made. Where energetically possible the v=1-4 reaction proceeds via a SS mechanism. The v=0 reaction most likely proceeds via a more intimate 3 body collision. Evidence shows that at high collision energies where SS is not allowed, the reaction competes with CID. New data are presented on the state selected $HD^+(v)$ reactions; the vibrational enhancement of the cross section for the HeD^+ channel falls off before that of HeH^+, in accordance with SS energetics. The larger cross sections for HeH^+ formation at low translational and higher vibrational energies seems to indicate the importance of the induced orientation of HD^+ due to the charge induced dipole interaction during the approach between HD^+ and He.

References

1. W. A. Chupka and M. E. Russell, J. Chem. Phys. 49, 5426 (1968)
2. W. A. Chupka, J. Berkowitz, and M. E. Russell, Sixth International Conference on the Physics of Electronic and Atomic Collisions, Abstracts of Papers, M. I. T. Press, Cambridge, 1969, pg. 71
3. J. A. Rutherford and D. A. Vroom, J. Chem. Phys. 58, 4076 (1973)
4. F. Schneider, U. Havemann, L. Zulicke, V. Pacak, K. Birkinshaw, and Z. Herman, Chem. Phys. Lett. 37, 323 (1976)
5. V. Pacak, U. Havemann, Z. Herman, F. Schneider, and L. Zulicke, Chem. Phys. Lett. 49, 273 (1977)
6. H. von Koch and L. Friedman, J. Chem. Phys. 38, 1115 (1963)
7. C. F. Giese and W. B. Maier II, J. Chem Phys. 39, 739 (1963)
8. R. H. Naynaber and G. D. Magnuson, J. Chem. Phys. 59, 825 (1973)
9. J. J. Leventhal, J. Chem. Phys. 54, 3279 (1971)
10. B. H. Mahan, J. Chem. Phys. 55, 1436 (1971)
11. F. Schneider and L. Zulicke, Chem. Phys. Lett. 67, 491 (1979)
12. P. J. Brown and E. F. Hayes, J. Chem. Phys. 55, 922 (1971)
13. P. J. Kuntz, Chem. Phys. Lett. 16, 581 (1972)
14. D. J. Kouri and M. Baer, Chem Phys. Lett. 24, 37 (1974)
15. J. T. Adams, Chem. Phys. Lett. 33, 275 (1975)
16. P. J. Kuntz and W. N. Whitton, Chem. Phys. Lett. 34, 340 (1975)
17. W. N. Whitton and P. J. Kuntz, J. Chem. Phys. 64, 3624 (1976)
18. C. Stroud, N. Sathyamurthy, R. Rangarajan, and L. M. Raff, Chem Phys. Lett. 48, 350 (1977)

19. N. Sathymurthy, J. W. Duff, C. Stroud, and L. M. Raff, J. Chem. Phys. 67, 3563 (1977)

20. N. Sathyamurthy, Chem. Phys. Lett. 59, 95 (1978)

21. D. R. McLaughlin and D. L. Thompson, J. Chem. Phys. 70, 2748 (1979)

22. N. Sathymurthy, Chem. Phys. 62, 1 (1981)

23. F. Schneider, U. Havemann, L. Zulicke, and Z. Herman, Chem. Phys. Lett. 48, 439 (1977)

24. J. C. Light and J. Lin, J. Chem. Phys. 43, 3209 (1965)

25. D. G. Truhlar, J. Chem. Phys. 56, 1481 (1972)

26. A. F. Wagner and D. G. Truhlar, J. Chem. Phys. 57, 4063 (1972)

27. K. T. Gillen, B. H. Mahan, and J. S. Winn, J. Chem. Phys. 59, 6380 (1973)

28. U. Havemann, V. Pacak, Z. Herman, F. Schneider, Ch. Zuhrt, and L. Zulicke, Chem. Phys. 28, 147 (1978)

29. J. C. Light, J. Chem. Phys. 41, 586 (1964)

30. J. C. Polanyi and W. H. Wong, J. Chem. Phys. 51, 1439 (1969)

31. M. J. Redmon and R. E. Wyatt, Chem. Phys. Lett. 63, 209 (1979)

32. D. M. Neumark, A. M. Wodtke, G. N. Robinson, C. C. Hayden, and Y. T. Lee, submitted to Phys. Rev. Lett. (1984)

Figure captions

FIG. 3.1. $H_2^+(v) + He \rightarrow HeH^+ + H$, Total cross section versus CM kinetic energy for v=0-4, raw cross sections shown. XBL 834-9164

FIG. 3.2. $H_2^+(v) + He \rightarrow HeH^+ + H$ Vibrational and translational energy dependence for HeH^+ formation, vibrationally corrected cross sections shown. XBL 833-8726

FIG. 3.3. $HD^+(v) + He \rightarrow HeD^+ + H$ Total cross section versus CM kinetic energy for v=0-4, raw cross sections shown. XBL 834-9160

FIG. 3.4. $HD^+(v=2) + He \rightarrow HeH^+ + D$ Total cross section versus CM kinetic energy, raw cross sections shown. XBL 8311-12314

FIG. 3.5. $HD^+(v=4) + He \rightarrow HeH^+ + D$ Total cross section versus CM kinetic energy using the old beam source, raw cross sections shown. XBL 839-11824

FIG. 3.6. Vibrational and translational energy dependence for the competition reactions of $HD^+ + He$ to form both HeH^+ and HeD^+, vibrationally corrected cross sections shown. XBL 842-736

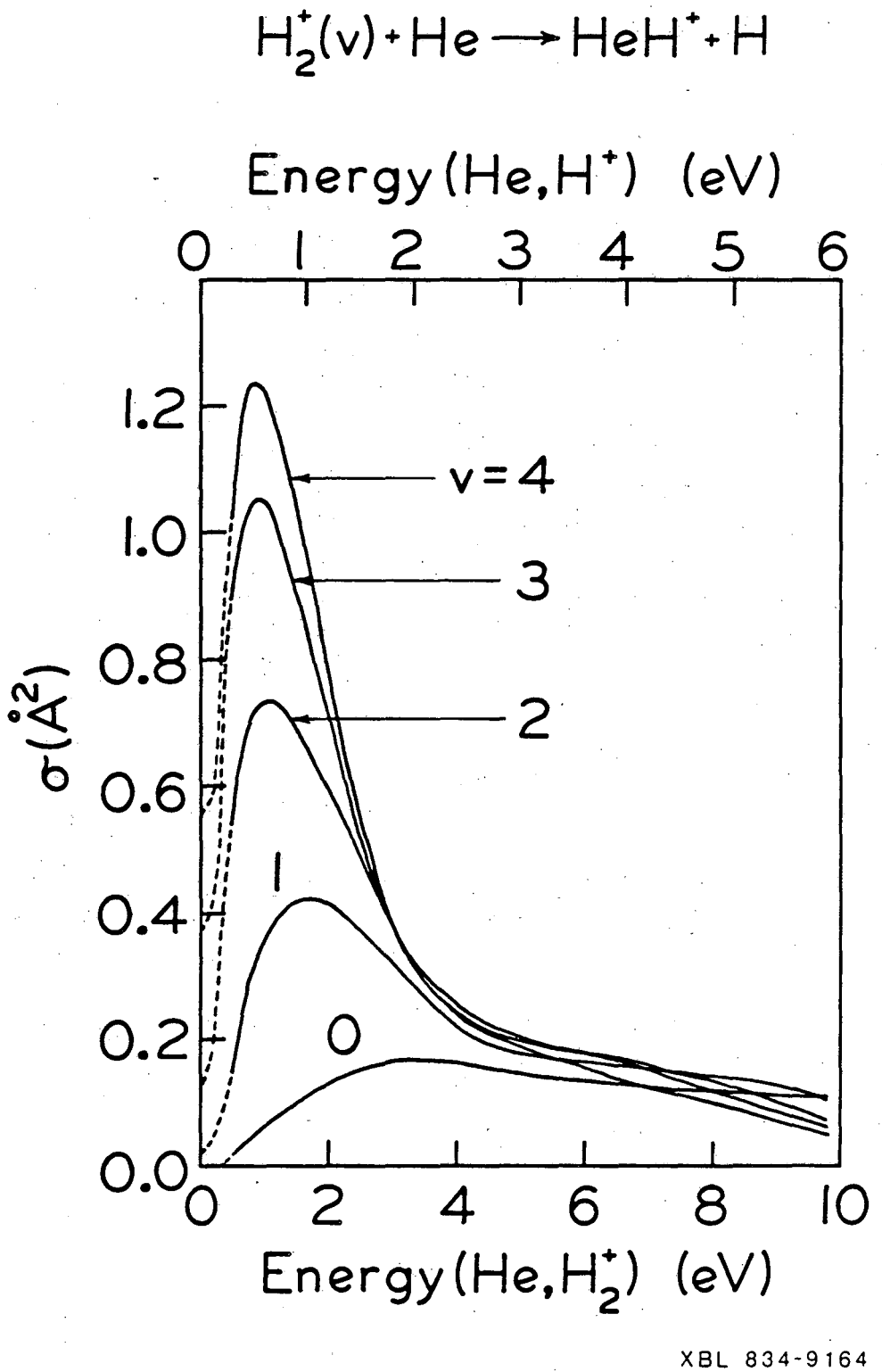
$H_2^+(v) + He \longrightarrow HeH^+ + H$
Energy(He,H+) (eV)
0 1 2 3 4 5 6
1.2
1.0
0.8
0.6
0.4
0.2
0.0
σ(Å²)
v=4
3
2
1
0
0 2 4 6 8 10
Energy(He,H₂+) (eV)
XBL 834-9164

Fig. 3.1

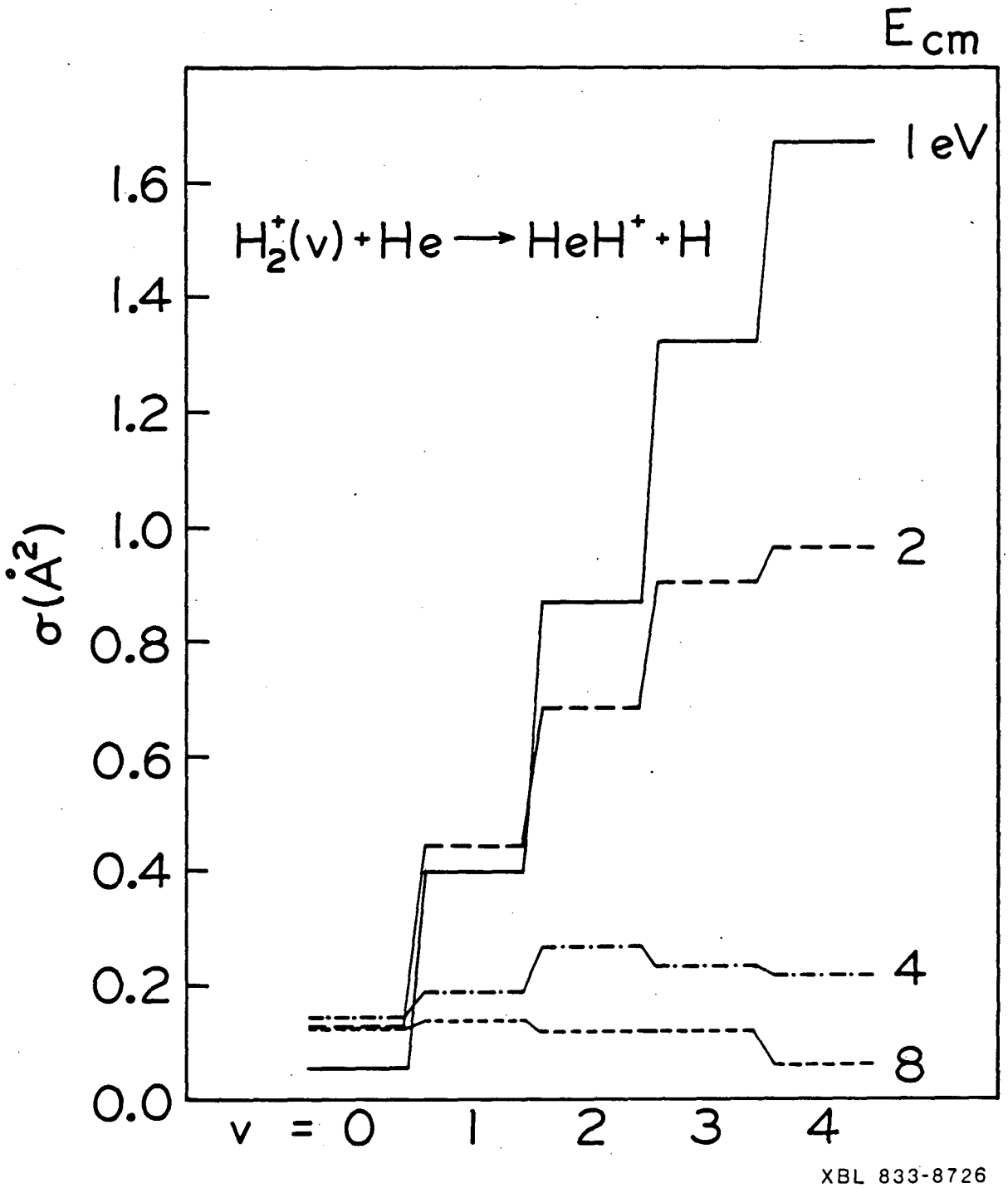
E cm
1 eV
2
4
8
$H_2^+(v) + He \rightarrow HeH^+ + H$
σ(Å²)
1.6
1.4
1.2
1.0
0.8
0.6
0.4
0.2
0.0
v = 0
1
2
3
4
XBL 833-8726

Fig. 3.2

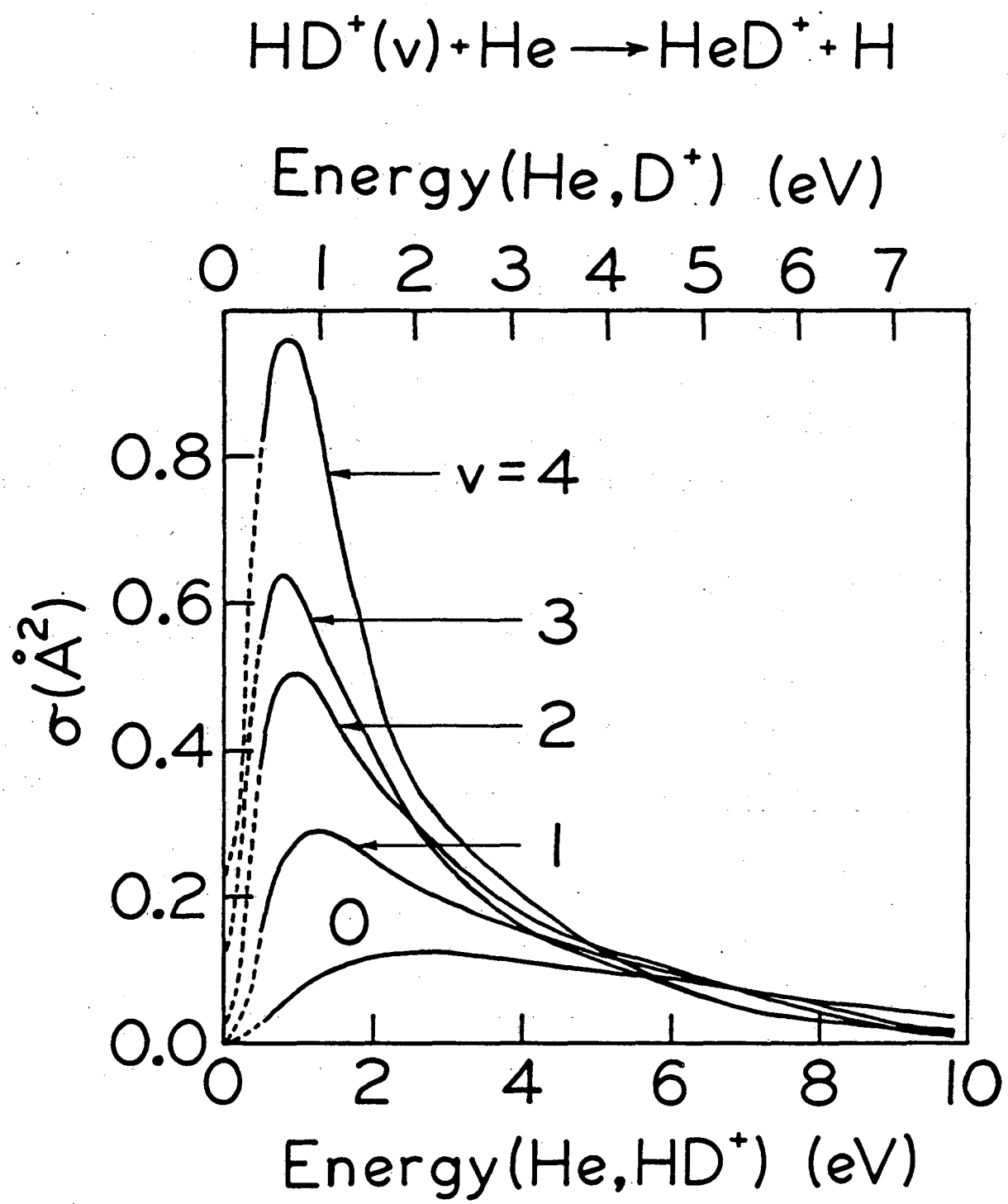

XBL 834-9160

Fig. 3.3

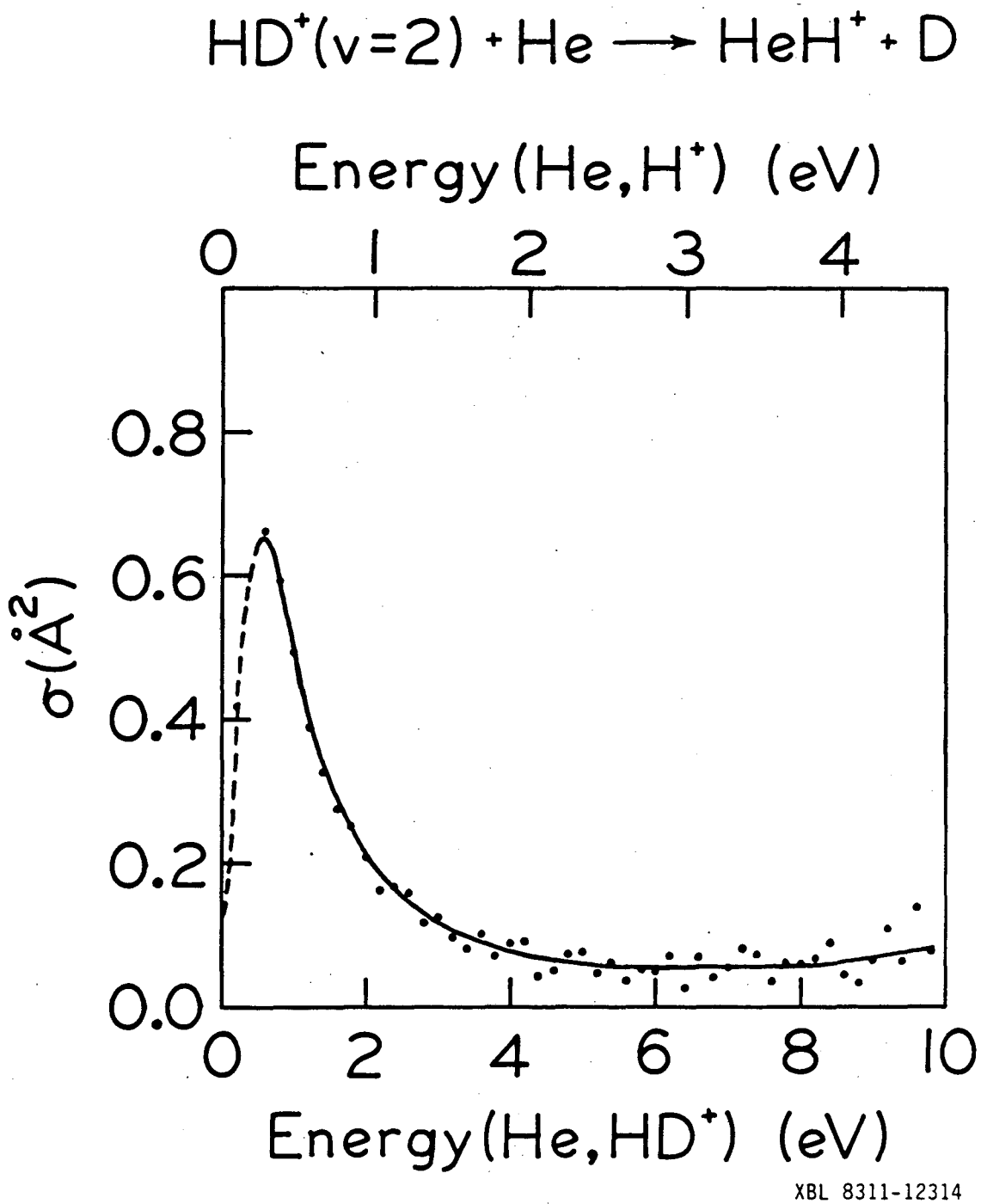

XBL 8311-12314

Fig. 3.4

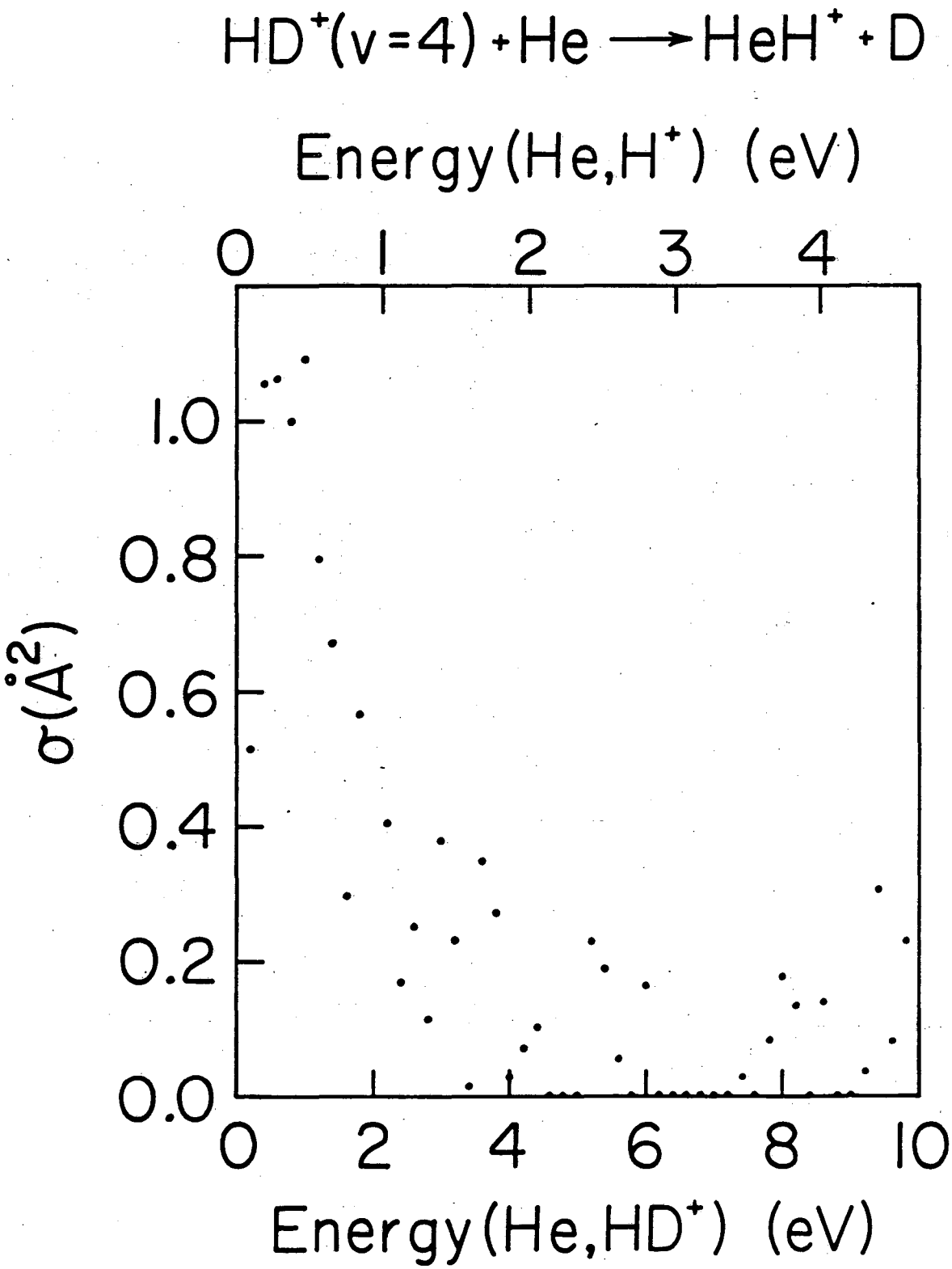

XBL 839-11824

Fig. 3.5

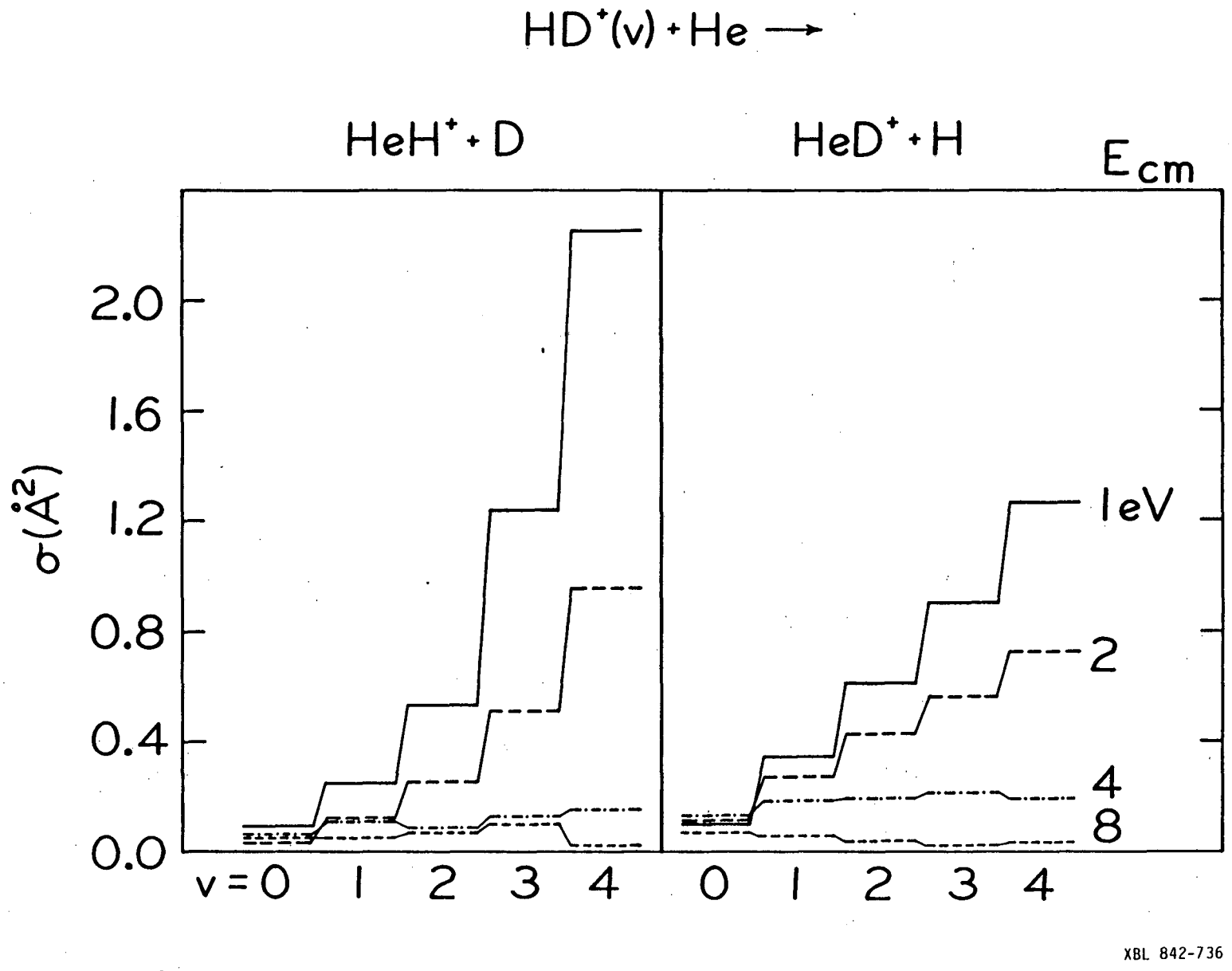
HD⁺(v) + He →
HeH⁺ + D
HeD⁺ + H
E cm
σ(Å²)
2.0
1.6
1.2
0.8
0.4
0.0
v = 0 1 2 3 4
0 1 2 3 4
1eV
2
4
8
XBL 842-736

Fig. 3.6

Tables

TABLE 3.1. Raw and vibrationally corrected data for $H_2^+(v) + He \rightarrow HeH^+ + H$. Cross sections given are $*10^{-1}$ Å^2.

	Raw				Deconvoluted			
Ecm/eV	1	2	4	8	1	2	4	8
v = 0	0.569	1.29	1.45	1.24	0.569	1.29	1.45	1.24
1	3.62	4.10	1.84	1.36	3.99	4.44	1.89	1.38
2	7.30	6.04	2.46	1.24	8.70	6.86	2.69	1.21
3	9.70	7.17	2.26	1.24	13.2	9.03	2.35	1.21
4	12.0	7.77	2.20	0.957	16.7	9.64	2.20	0.624

TABLE 3.2. Raw and vibrationally corrected data for the $HD^+ + He \rightarrow HeH^+, HeD^+ + D,H$ reactions. Cross sections given are $*10^{-1}$ Å^2.

		HeH^+				HeD^+			
	Ecm/eV	1	2	4	8	1	2	4	8
	v = 0	0.989	0.340	0.627	0.464	1.01	1.16	1.27	0.698
	1	2.26	1.19	1.03	0.531	3.10	2.44	1.75	0.574
Raw	2	4.93	2.05	0.893	0.639	4.97	3.56	1.85	0.437
	3	8.55	3.57	1.10	0.819	6.81	4.45	1.94	0.335
	4	12.8	5.41	1.23	0.537	8.38	5.18	1.87	0.368
	Ecm/eV	1	2	4	8	1	2	4	8
	v = 0	0.989	0.340	0.627	0.464	1.01	1.16	1.27	0.698
	1	2.47	1.33	1.09	0.542	3.44	2.65	1.83	0.554
Deconvoluted	2	6.36	2.56	0.870	0.699	6.11	4.24	1.94	0.357
	3	12.4	5.13	1.26	1.00	9.01	5.60	2.08	0.203
	4	22.5	9.55	1.56	0.250	12.6	7.25	1.86	0.313

TABLE 3.3. Energies for which the proton transfer reaction is allowed via spectator stripping.

$v(H_2^+)$	HeH^+	$v(HD^+)$	HeH^+	HeD^+
0	1.33–4.42eV	0	1.76–5.72eV	1.05–3.43eV
1	0.88–3.97	1	1.24–5.21	0.75–3.12
2	0.45–3.53	2	0.75–4.71	0.45–2.83
3	0.05–3.13	3	0.24–4.20	0.14–2.52
4	0.00–2.77	4	0.00–3.69	0.00–2.21

Introduction

The effect of vibrational and translational energy on the reaction cross section for endothermic atom-diatom systems is fairly well understood with respect to the location of the barrier along the reaction coordinate on a potential energy surface (PES).[1] Generally, translational energy is more effective than vibrational energy in driving the reaction if the barrier to the reaction is encountered early on the PES. If the barrier is found late in the exit channel, then vibrational energy is more effective than the same amount of energy present as translation in driving the reaction. The $H_2^+ + He \rightarrow HeH^+ + H$ reaction is characterized by this latter case.[2]

For an endothermic reaction between two molecules, the effect of translational and vibrational excitation on the reaction cross section is somewhat more complicated. There are many ways of adding vibrational energy in polyatomic molecules and in contrast to atom-diatom systems, added vibrational energy is not necessarily coupled directly to the reaction coordinate. The trends seen for these larger systems may be expected to be qualitatively the same as those seen for the atom-diatom systems if the reaction is a simple atom transfer reaction and the vibrational energy is added to the bond being broken. But the effect vibrational energy has in promoting an endothermic reaction might not be appreciable if the excited vibrational degree of freedom is not coupled directly to the reaction coordinate.

Relatively few endothermic reactions involving polyatomic systems containing 4 or more atoms have been studied as a function collision

and vibrational energy. Krajnovich, et. al. have carried out such a study on the Br + $CF_3I \rightarrow CF_3$ + IBr reaction by the crossed molecular beams method; highly vibrationally excited CF_3I was prepared by the infared multiphoton excitation process and a beam of hyperthermal Br atoms was produced by seeded supersonic expansion.[3] Two trends could be related to generalizations obtained from the results of classical scattering calculations on endothermic atom transfer reactions. The amount of forward scattered IBr (with respect to the initial Br direction) increases with vibrationally hot CF_3I as compared to vibrationally cold CF_3I in accord with previous trajectory calculations.[4] When the collision energy is comparable to the endoergic barrier height, vibration is substantially more effective than translation in promoting the reaction partially due to constraints imposed by the conservation of angular momentum of the system. However, when the collision energy is several times the barrier height, vibrational energy appears to be less effective than an equivalent amount of translational energy in driving the reaction suggesting that the PES has a gradual barrier with most of the barrier lying in the entrance channel.[5] The comparison of vibrational to translational energy in this experiment was only qualitative as the extent of vibrational excitation of the CF_3I could only be estimated for the multiphoton absorption process.

In a molecule-molecule reaction, a chemical bond which is not to be broken but is coupled to the reaction coordinate may be excited. Duncanson and Guillory reacted CH(v=0,1) with N_2 presumably to form the products HCN and N.[6] The HCN + N product channel is the least

endothermic reaction channel for v=0 and becomes exothermic for v=1. The rate of disappearance of CH increased by a factor of 40 from v=0 to v=1 as determined from the decay rate of CH monitored by LIF. Although the substantial increase of the disappearance rate of CH(v=1) over CH(v=0) could be due to the enhanced reactivity, neither the HCN product formation nor the increase of CH(v=0) due to vibrational relaxation of CH(v=1) was monitored directly; the relative contributions of reaction and vibrational relaxation to the decay rate of CH are not known.

Experiments have shown the $H_2 + D_2 \rightarrow 2HD$ metathesis reaction to proceed with vibrational energy added to either H_2 or D_2.[7,8] Ab initio studies, however, predict an activation barrier well above the H_2 bond energy for this reaction.[9] The reaction of $NO + O_3 \rightarrow NO_2 + O_2$ has been shown to overcome its activation barrier with vibrational excitation in either of the reactants.[10,11]

The excitation of the C-C stretching vibration in $C_2H_2^+$ in promoting the H atom transfer reaction of $C_2H_2^+ + H_2 \rightarrow C_2H_3^+ + H$ has proven itself interesting. The reaction is endothermic for ground state reactants and becomes exothermic for $C_2H_2^+$ in its first excited vibrational state. Photoionization appearance potentials of reactants and products set the ground state reaction endothermicity close to 1 kcal/mole.[12-17] Buttrill, et al. studied this reaction by both photoionization and ion cyclotron resonance (ICR) techniques.[18] A photoionization mass spectrometer arrangement was used to examine the reaction cross sectional dependence on ion vibrational energy, however, only at

thermal collision energies. The reaction was found to be strongly vibrationally enhanced for v=0-2 at this collision energy. The ICR experiment was used to measure an absolute rate for this reaction averaged over all the vibrational states produced in the electron impact ionization of C_2H_2. A value of $6.3 \pm 1.8 \times 10^{-11}$ cm^3 $molecule^{-1}$ sec^{-1} was obtained. No evidence was found to support a long lived complex mechanism for this reaction. In a more recent study, Adams and Smith estimate a thermal reaction rate of 7.0×10^{-11} cm^3 $molecule^{-1}$ sec^{-1} using their SIFT apparatus,[19] in close agreement with Buttrill's experiment.

In this paper results obtained using our unique apparatus consisting of a photoionization ion source and octapole RF ion guide to study the $C_2H_2^+(v) + H_2$ system are described. The reaction cross section for this system was measured as a function of both ion vibrational and translational energy for the purpose of making a comparison between vibrational energy and translational energy in driving an endoergic reaction, especially for a larger polyatomic system where vibrational energy is added to a part of the molecular system which might be only weakly coupled to the reaction coordinate. When the H atom transfers from H_2 to $C_2H_2^+$, the H-H bond is ruptured and a new C-H bond is formed. Although the acetylene ion C-C bond appears to remain intact, the formation of the new C-H bond could reduce the bond order and lengthen the C-C bond and its stretching vibration could be a part of the reaction coordinate. The 50-750 meV center of mass (CM) kinetic energy range used here extends the knowledge derived from previous thermal studies.

Results and Analysis

Figure 4.1 shows the raw relative reaction cross sections as a function of vibrational and kinetic energy. Because the scattering cell pressure was not accurately calibrated and measured, the total absolute cross section was not measured. However, the total absolute reaction cross section in its raw form is estimated from ion gauge pressure measurements near the scattering cell to be approximately 1 $Å^2$ at its maximum value. The cross section for v=0 is normalized to the thermal rate constant as measured by Adams and Smith.[14] Their reported rate constant is 1.0×10^{-11} cm^3 $molecule^{-1}$ sec^{-1} which cooresponds to an average cross section of 0.54 Å to which the 50 meV, v=0 cross section of this experiment is normalized. Figure 4.2 shows the data of Figure 4.1 after the raw cross sections have been vibrationally deconvoluted. All collision energies are for the CM frame unless otherwise specified. At 50 meV collision energy the reaction is strongly vibrationally enhanced. The relative cross section increases from 1.00 to 5.72 at 50 meV, v=0-2. As the collision energy is increased, the vibrational enhancement becomes less pronounced. The v=0-1 step decreases monotonically from 50-750 meV; however the v=1-2 step decreases with energy until 250 meV when the v=1-2 step gradually increases.

Figure 4.3 is a plot of the raw relative reaction cross section as a function of collision energy for $C_2H_2^+(v=0)$. The cross section shows a monotonic increase from 100-750 meV. Figure 4.4 is a plot of the raw relative reaction cross section as a function of collision

energy for $C_2H_2^+$ produced at 1034 Å which consists of v=0-2 vibrational states. For the energy range covered in this experiment, the measured cross section is highest at 50 meV and rapidly decreases thereafter. This rapid decline is real and reflects the strong vibrational enhancement of the cross section from v=0-2 at low collision energies. The cross section levels off from 100-400 meV at which time it slowly starts to climb. At 750 meV, the cross section is roughly 30 percent greater than its minimum value. The cross section basically shows slight translational dependence beyond 100 meV. The wavelength scans at different collision energies are all normalized to this energy scan. Table 4.1 gives the values of the cross section as a function of kinetic and vibrational energy for both the raw and vibrationally deconvoluted data normalized to the data found in Figure 4.4. Table 4.2 gives the values of the cross section as a function of vibrational energy only; the v=0 cross sections are normalized to 1.00 at each collision energy. This table also gives the vibrational step cross section ratio for v=2-1.

Upon vibrationally deconvoluting the data, cross sectional trends seen in the raw data can become enormously magnified because of the enormous contribution of v=0 at each selected wavelength. Small errors in the raw data can result in large errors upon deconvolution and can greatly influence interpretation and analysis of the deconvoluted data. For this reason both the raw and vibrationally deconvoluted data are reported.

Discussion

Although the uncertainty of the estimated heat of reaction of $C_2H_2^+ + H_2 \rightarrow C_2H_3^+ + H$ is larger than the estimated endothermicity, the experimental results of this reaction appears to be in agreement with what is expected for a slightly endothermic reaction. Combining the well defined ionization potential for C_2H_2 of 11.402 eV[12] with the well known heat of formation of $\Delta H^0_{f\ 298}(C_2H_2)$=2.350 eV[20] one calculates $\Delta H^0_{f\ 298}(C_2H_2^+)$=13.752 eV. The heat of formation of $C_2H_3^+$ is less well defined, however, as its appearance threshold from the dissociative photoionization of C_2H_4 is not well determined and is estimated by Chupka, et al. to be 13.25 ± 0.05 eV as an upper limit.[21] Using $\Delta H^0_{f\ 298}(C_2H_4)$=0.544 eV[20] one may calculate $\Delta H^0_{f\ 298}(C_2H_3^+)$=11.535 eV. The above chemical reaction then simply has an upper limit to its endothermicity of 42 meV at 298°K. Taking Chupka's other possible appearance potential for $C_2H_3^+$ of 13.13 ± 0.02 eV,[21] one arrives at a reaction exothermicity of -78 meV. This threshold is less well defined and is not consistent with our experimental observations.

The data presented here, at a relative collision energy of 50 meV shows an enhancement of the reaction cross section of over a factor of 5 for increasing C-C stretching vibration in $C_2H_2^+$ from v=0 to v=2. The substantial vibrational enhancement is in qualitative agreement with the previous study of Buttrill, et. al.[18] However, as the collision energy is raised, the vibrational enhancement of the reaction cross section declines. Energy partitioned into the translational degree of freedom between the reactants is seen to only slightly

enhance the reaction compared to the vibrational enhancement; over the energy range covered, the cross section for $C_2H_2^+(v=0)$ increases only about a factor of two from its minimum to maximum values as seen in Figure 4.3.

Experimentally this $C_2H_2^+(v) + H_2$ reaction behaves in many ways similarly to the $H_2^+(v)$ + He reaction.[2] In the $H_2^+(v)$ + He reaction, one is exciting the bond which is to be broken. Both v=0 reactions show little translational energy dependence. The $H_2^+(v=0)$ reaction probably proceeds through intimate, small impact parameter collisions. At low collision energies the H_2^+ + He reaction is strongly vibrationally enhanced. Vibrational energy along the reaction coordinate strongly promoting the reaction over translational energy is indicative of a barrier found late in the exit channel of the PES.[1] Collision energy being less effective than an equivalent amount of vibrational energy even up to several times the barrier height suggests that the barrier lies mostly in the exit channel of the PES.[5] The failure of translational energy in promoting the reaction of $C_2H_2^+(v=0)$ efficiently clearly suggests that the potential energy barrier associated with the C-H bond formation and H-H bond rupture is late along the reaction coordinate, similar to the H_2^+ + He reaction.

In an earlier study using the photoionization mass spectrometer technique, Buttrill, et al. found that the cross section is enhanced over an order of magnitude when the C-C stretching vibration is increased from v=0-2; the vibrationally corrected relative cross sections for v=0: 1: 2 are 1.0: 6.0: 12.[18] Buttrill attributes the

appreciable reactivity of the endothermic reaction of $C_2H_2^+(v=0)$ at thermal energies to the thermal excitation of the lower frequency bending modes. At room temperature it was estimated that 14 percent of the C_2H_2 molecules have one quanta of vibration in either of the dou

bly degenerate ν_4 or ν_5 bending modes (76 and 90 meV respectively).[22] Assuming the energy of these modes remains the same for the ion as the neutral upon photoionization, this residual vibrational energy is above the calculated reaction endothermicity and would be able to drive the v=0 reaction. But whether only those $C_2H_2^+$ molecules with one quanta of bending excitation are responsible for the thermal energy reaction of $C_2H_2^+(v=0)$ is not clear. At 300°K, the average translational energy between collision pairs is 39 meV. A large fraction of molecules have enough relative collision energy to drive the reaction even without the thermal excitation of the bending vibrations or rotational degrees of freedom.

McClelland, et. al.[23] and Mariella, et. al.[24] studied the effect of vibrational relaxation of diatomic molecules in seeded supersonic beams. They studied the relaxation processes for I_2 and LiF respectively. The I_2 vibrational energy spacing is 214 cm^{-1} and that of LiF is 910 cm^{-1}.[25] In both cases the molecules were substantially relaxed upon supersonic expansion with up to a 40 percent decrease in vibrational temperature. In our experiment $C_2H_2^+$ was produced by photoionization of a supersonic beam of C_2H_2 and the ν_4 and ν_5 vibrational modes of $C_2H_2^+$ (612 and 729 cm^{-1} respectively) are expected to substantially relax during the isentropic expansion. Consequently most

of the product seen from the v=0, $C_2H_2^+$ ions in this experiment is expected to be the actual reaction of v=0 ions.

Buttrill and co-workers further investigated the reaction of $C_2H_2^+$, formed with the electron impact of 15 eV electrons, with D_2 at thermal collision energies. Since no $C_2D_2H^+$ ions were detected at low D_2 pressures, the conclusion was reached that the a long-lived intermediate $C_2H_2D_2^+$ complex does not play any role as a reaction mechanism. A rate constant of $6.3 \pm 1.8 \times 10^{-11}$ cm^3 $molecule^{-1}$ sec^{-1} which represents an average over the distribution of vibrationally excited $C_2H_2^+$ molecules reacting with H_2 was measured. Adams and Smith report agreement with this rate constant using their SIFT apparatus at room temperature.[19] The thermalized $C_2H_2^+$ molecules are reacted with H_2 and a rate constant of 1.0×10^{-11} cm^3 $molecule^{-1}$ sec^{-1} was measured. Using Buttrill's argument they say 14 percent of the $C_2H_2^+$ molecules at room temperature have one vibrational quanta in either the ν_4 or ν_5 mode which are responsible for the formation of $C_2H_3^+$. The estimated rate coefficient for these excited state reactions is more like 7×10^{-11} cm^3 $molecule^{-1}$ sec^{-1} in agreement with the value of Buttrill, et al. In fact at a temperature of 300°K and using a value of 76 and 90 meV for the doubly degenerate ν_4 and ν_5 modes respectively, one calculates that 8 percent of the total number of $C_2H_2^+$ molecules have one quanta in either of these two modes instead of 14 percent. Adams and Smith perform their experiment in a flow tube which guarantees all reactants to have a Boltzmann vibrational population distribution due to the collisional quenching of the higher vibrational levels by the

carrier gas before reactions can take place. Thus the measured rate is for $C_2H_2^+(v=0)$ with some excitation in the ν_4 and ν_5 bending modes, but without those $C_2H_2^+$ which have one and two quanta in the C-C stretching vibration. The rate constants measured in each experiment are not the same and the reported closeness of their values is entirely based on the assumption that ground state $C_2H_2^+$ does not react at thermal energy which is not at all convincing.

The PES for this reaction has not been previously calculated. Electronically excited and charge transfer states are not expected to play a role in this reaction because the first electronic state of $C_2H_2^+$ above the $X^2\pi_u$ ground state is 4.96 eV higher in energy. The difference in the ionization potentials (IP) between C_2H_2 and H_2 puts the charge exchanged system of reactants, $C_2H_2 + H_2^+$, 4.02 eV higher than ground state reactants. Based on the IP of C_2H_4 of 10.51 eV[26] and $\Delta H^0_{f\ 298}(C_2H_4)$=0.544 eV,[20] the potential well cooresponding to the $C_2H_4^+$ complex is 2.698 eV below reactants. Apparently this potential well cannot be accessed from the ground states of $C_2H_2^+$ and H_2 under our experimental conditions. A large potential barrier must exist between $C_2H_4^+$ and $C_2H_2^+ + H_2$.

The electronic configuration of the $X^2\pi_u$ ground state of $C_2H_2^+$ is $(1\sigma_g)^2(1\sigma_u)^2(2\sigma_g)^2(2\sigma_u)^2(3\sigma_g)^2(1\pi_u)^3$ where one lone electron is found in one of the degenerate $1\pi_u$ molecular orbitals. The $1\pi_u$ orbital is formed from a combination of $2p_x$ and $2p_y$ atomic orbitals of the C atoms with the $2p_z$ orbital defined as lying along the internuclear axis. This electron is shared equally between the two C atoms. As

H_2 approaches the $C_2H_2^+$ molecule, the electron cloud along the C-C bond distorts and H atom addition to one C atom should localize the lone electron to that C atom and localize the positive charge on the other C atom unless the bridged structure with one H atom bridging the two C atoms is more stable. As one of the H atoms in the H_2 molecule continues to approach the extended C-C bond, the electron becomes more and more localized. The C-C bond of $C_2H_3^+$ should resemble the double bond of C_2H_4. Since the bond order of $C_2H_2^+$ is 2-1/2 as compared to 2 for $C_2H_3^+$, one would expect the bond length of $C_2H_3^+$ to be slightly longer than that of $C_2H_2^+$. H atom addition to $C_2H_2^+$ in its ground vibrational state v=0 will accompany a cooresponding increase in the C-C bond distance and the C-C stretching vibration is indeed coupled directly to the reaction coordinate. With $C_2H_2^+$ in an excited vibrational state, C-H bond formation would be facilitated by the extension of the C-C bond. Consequently vibrational energy would serve to effectively lower the barrier to reaction and one would see a vibrational enhancement to the reaction.

Apparently vibrational energy in the C-C bond is quite effective in driving the $C_2H_2^+ + H_2$ reaction over its barrier, especially at low collision energies. Simplistically the C-C bond does not appear to play an important role in this reaction; the H_2 bond must be severed and a C-H bond must be formed. However, the reaction coordinate is apparently not so simple as for the H_2^+ + He case. For the present reaction, as the H_2 bond is breaking and the new C-H bond is forming, the C-C bond must stretch to accomodate these changes. Thus the

reaction coordinate involves the concerted motion of the four H-H-C-C atoms. The stretching motion of the C-C bond seems to be as important as that of the H-H bond for the H atom transfer.

References

1. J. C. Polanyi and W. H. Wong, J. Chem. Phys. 51, 1439 (1969)
2. T. Turner, O. Dutuit, and Y. T. Lee, J. Chem. Phys. (1984) to be published.
3. D. Krajnovich, Z. Zhang, F. Huisken, Y. R. Shen, and Y. T. Lee, Twelfth International Conference on the Physics of Electronic and Atomic Collisions, Gatlinburg, 1981.
4. D. S. Perry, J. C. Polanyi, C. W. Wilson, Jr., Chem Phys. 3, 317 (1974)
5. J. C. Polanyi and N. Sathyamurthy, Chem. Phys. 33, 287 (1978)
6. J. A. Duncanson and W. A. Guillory, J. Chem. Phys. 78, 4958 (1983)
7. S. H. Bauer and E. Ossa, J. Chem. Phys. 45, 434 (1966)
8. S. H. Bauer, D. M. Lederman, E. L. Resler. Jr., and E. R. Fisher, Int. J. Chem. Kinet. 5, 93 (1973)
9. D. M. Silver, J. Chem. Phys. 59, 3378 (1973)
10. K. K. Hui and T. A. Cool, J. Chem. Phys. 68, 1022 (1978)
11. J. C. Stephenson and S. M. Freund, J. Chem. Phys. 65, 1893 (1976)
12. V. H. Dibeler, J. A. Walker, and K. E. McColloh, J. Chem. Phys. 59, 2264 (1973)
13. W. A. Chupka, J. Berkowitz, and K. M. A Refaey, J. Chem. Phys. 50, 1938 (1969)
14. V. H. Dibeler, and J. A. Walker, Int. J. Mass Spec. Ion Phys. 11, 49 (1973)
15. I. Omura, T. Kaneko, Y. Yamada, and K. Tanaka, J. Phys. Soc. Japan 27, 178 (1969)

16. V. H. Dibeler, J. A. Walker, and H. M. Rosenstock, J. Phys. 44, 1271 (1966)

17. Y. Ono, E. A. Osuch, and C. Y. Ng, J. Chem. Phys. 76, 3905 (1982)

18. S. E. Bruttrill Jr., J. K. Kim, W. T. Huntress Jr., P. LeBreton, and A. Williamson, J. Chem. Phys. 61, 2122 (1974)

19. N. G. Adams and D. Smith, Chem. Phys. Lett. 47, 383 (1977)

20. D. R. Stull, H. Prophet, et al. JANAF Thermochemical Tables, Second Edition. NSRDS-NBS 37, National Bureau of Standards, 1971. The conversion 23.06 kcal/mole = 1.000 eV/molecule is used throughout this paper.

21. W. A. Chupka, J. Berkowitz, and K. M. A. Refaey, J. Chem. Phys. 50, 1939 (1969)

22. G. Herzberg, Molecular Spectra and Molecular Structure III Electronic Spectra and Electronic Structure of Polyatomic Molecules, Van Nostrand Reinhold Co., N.Y., 1966, pg. 611.

23. G. M. McClelland, K. L. Saenger, J. J. Valentini, and D. R. Herschbach, J. Phys. Chem. 83, 947 (1979)

24. R. P. Mariella, Jr., S. K. Neoh, D. R. Herschbach, and W. Klemperer, J. Chem. Phys. 67, 2981 (1977)

25. K. P. Huber and G. Herzberg, Molecular Spectra and Molecular Structure IV Constants of Diatomic Molecules, Van Nostrand Reinhold Co., N.Y., 1979, pgs. 332 and 380.

26. J. Berkowitz, Photoabsorption, Photoionization, and Photoelectron Spectroscopy, Academic Press, N. Y., 1979, pg.291.

Figure Captions

FIG. 4.1. $C_2H_2^+(v) + H_2 \rightarrow C_2H_3^+ + H$. Vibrational and translational energy dependence for $C_2H_3^+$ formation. Raw relative cross sections shown. The cross sections are normalized to 0.541 for v=0, 50 meV as described in the text. XBL 846-2620

FIG. 4.2. $C_2H_2^+(v) + H_2 \rightarrow C_2H_3^+ + H$. Vibrational and translational energy dependence for $C_2H_3^+$ formation. Relative cross sections shown are deconvoluted from the raw data of Figure 4.1 using the vibrational distribution of $C_2H_2^+$ given in Table 2.2. XBL 846-2584

FIG. 4.3. $C_2H_2^+(v=0) + H_2 \rightarrow C_2H_3^+ + H$. Total cross section versus CM kinetic energy obtained at the wavelength chosen to produce v=0, raw cross sections shown. XBL 846-2387

FIG. 4.4. $C_2H_2^+(v=0\text{-}2) + H_2 \rightarrow C_2H_3^+ + H$. Total cross section versus CM kinetic energy obtained at the wavelength chosen to produce v=0-2, raw cross sections shown. XBL 846-2588

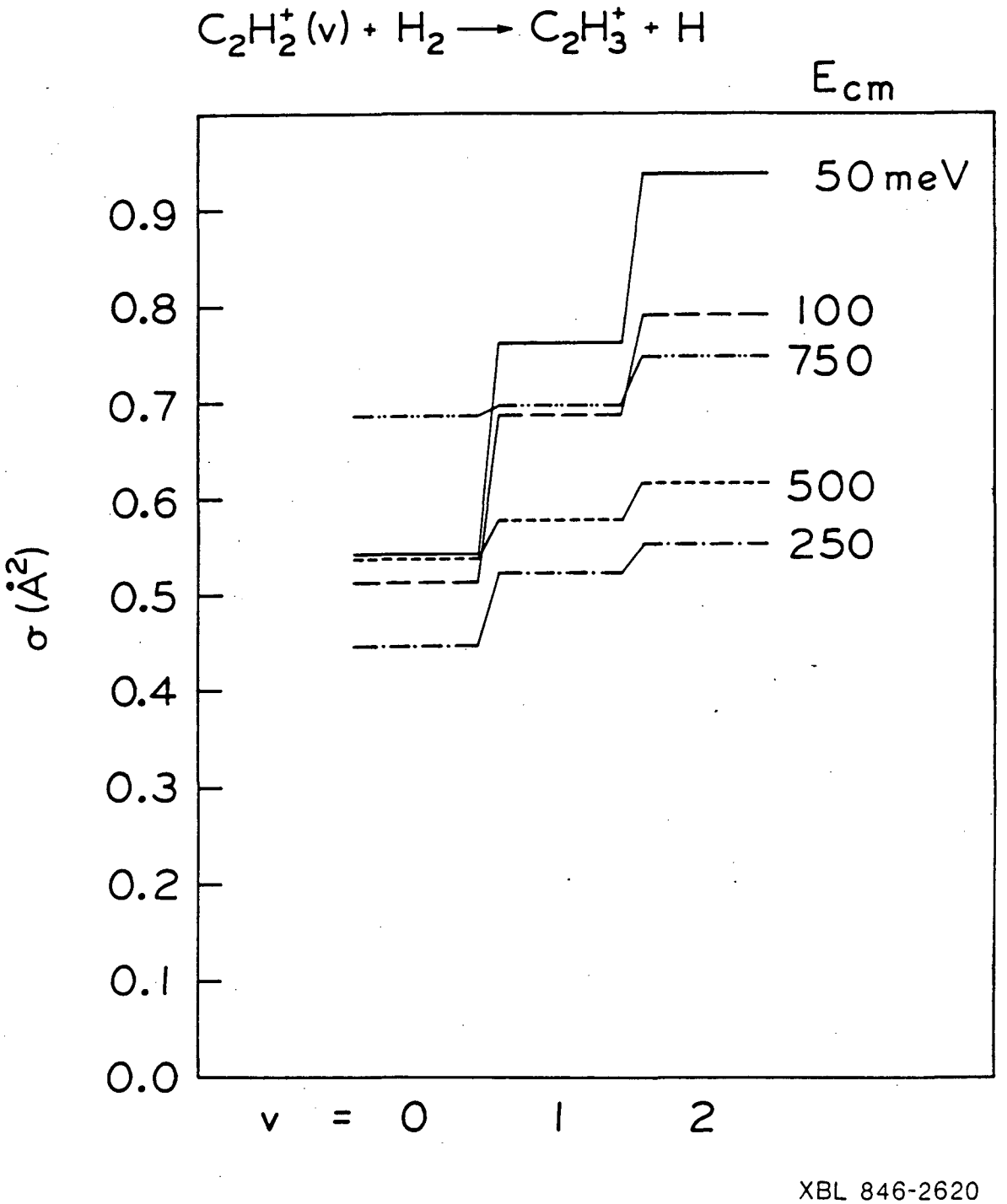
$C_2H_2^+(v) + H_2 \longrightarrow C_2H_3^+ + H$
E_{cm}
50 meV
100
750
500
250
0.9
0.8
0.7
0.6
0.5
0.4
0.3
0.2
0.1
0.0
σ (Å²)
v = 0 1 2
XBL 846-2620

Fig. 4.1

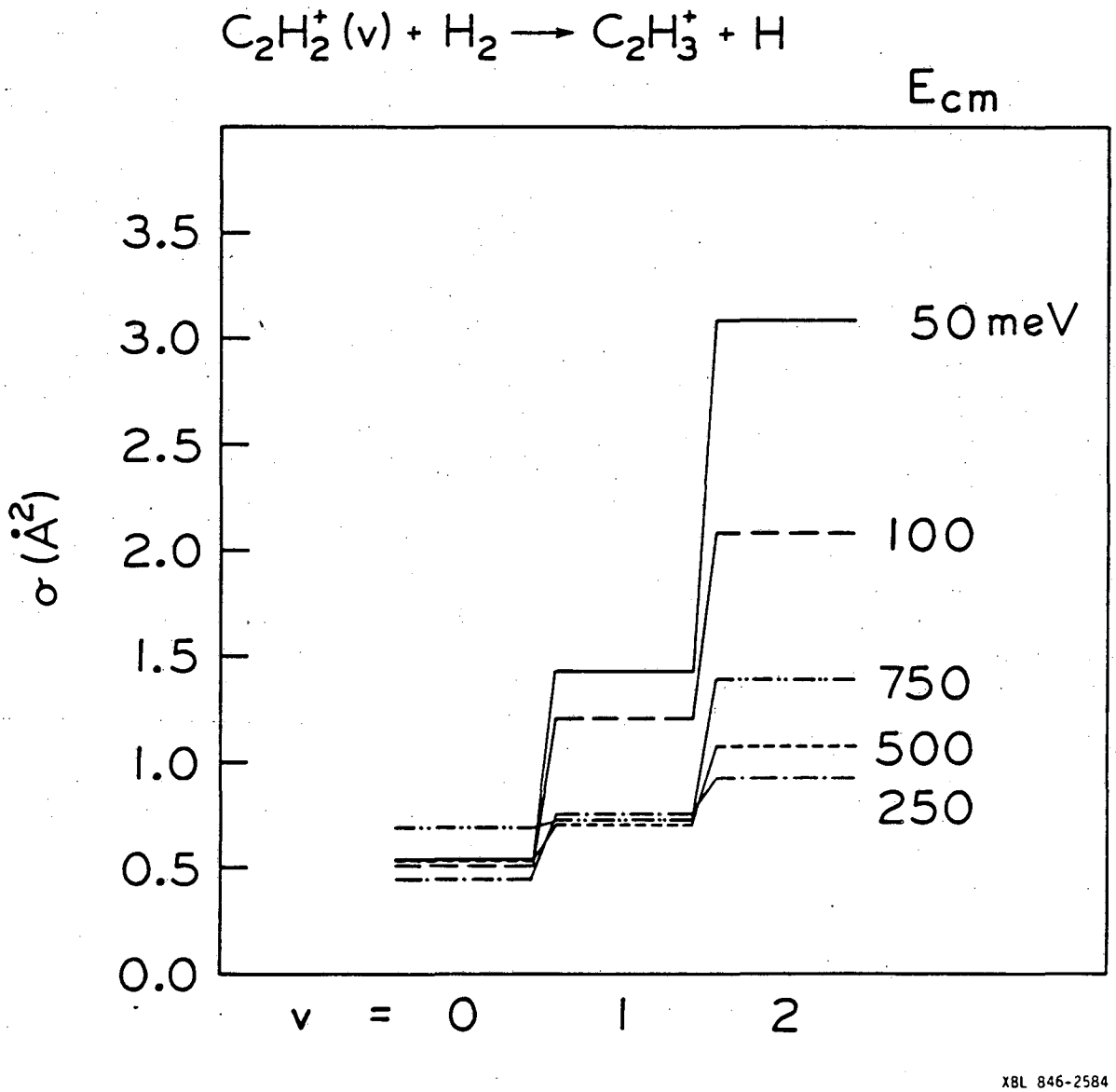
$C_2H_2^+(v) + H_2 \longrightarrow C_2H_3^+ + H$
E_{cm}
3.5
3.0
2.5
2.0
1.5
1.0
0.5
0.0
σ (Å²)
50 meV
100
750
500
250
v = 0 1 2
XBL 846-2584

Fig. 4.2

$$C_2H_2^+(v=0) + H_2 \longrightarrow C_2H_3^+ + H$$

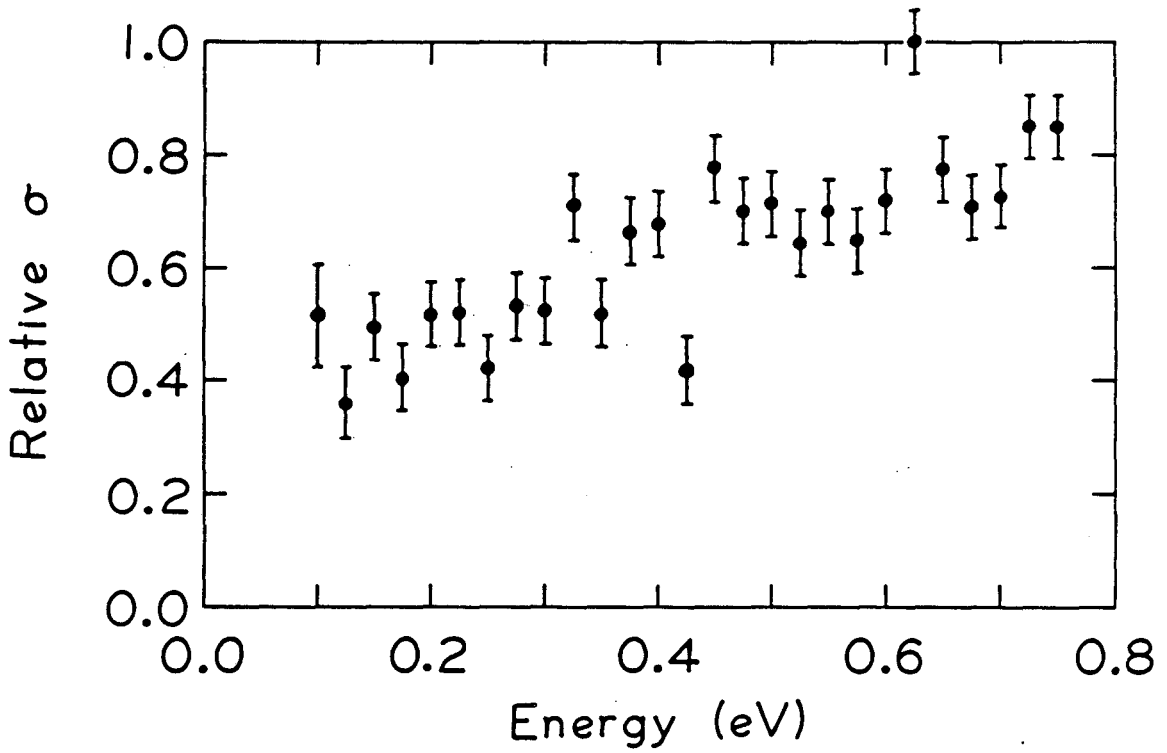

XBL 846-2387

Fig. 4.3

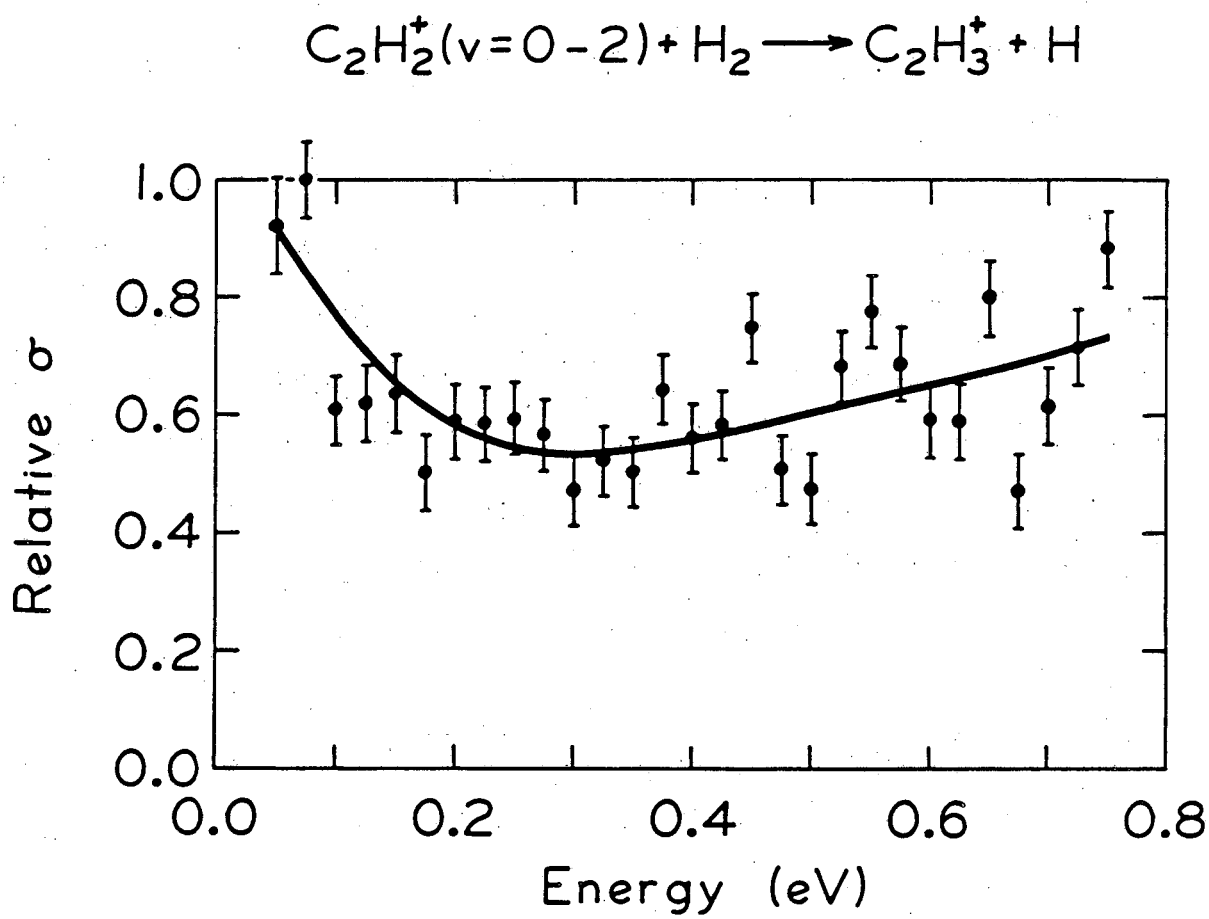

XBL 846-2588

Fig. 4.4

Tables

Table 4.1. Raw and vibrationally corrected data for $C_2H_2^+(v) + H_2 \rightarrow C_2H_3^+ + H$. Cross sections are normalized relative to the v=0, 50 meV cross section as 0.541 as described in the text.

	Raw			Deconvoluted		
E_{cm}	v=0	1	2	0	1	2
50 meV	0.541	0.762	0.938	0.541	1.43	3.09
100	0.512	0.686	0.791	0.512	1.21	2.08
250	0.447	0.523	0.554	0.447	0.754	0.932
500	0.537	0.578	0.616	0.537	0.704	1.08
750	0.687	0.697	0.748	0.687	0.726	1.39

Table 4.2. Vibrationally corrected data for $C_2H_2^+(v) + H_2 \rightarrow C_2H_3^+ + H$ with all v=0 cross sections normalized to 1.00. Total cross sections and the cross section ratio for v=2: v=1 are given.

E_{cm}	v=0	1	2	v=2:v=1
50 meV	1.00	2.64	5.72	2.16
100	1.00	2.38	4.07	1.71
250	1.00	1.69	2.08	1.24
500	1.00	1.31	2.02	1.54
750	1.00	1.06	2.02	1.91

This report was done with support from the Department of Energy. Any conclusions or opinions expressed in this report represent solely those of the author(s) and not necessarily those of The Regents of the University of California, the Lawrence Berkeley Laboratory or the Department of Energy.

Reference to a company or product name does not imply approval or recommendation of the product by the University of California or the U.S. Department of Energy to the exclusion of others that may be suitable.

TECHNICAL INFORMATION DEPARTMENT
LAWRENCE BERKELEY LABORATORY
UNIVERSITY OF CALIFORNIA
BERKELEY, CALIFORNIA 94720